Petrology and geochemistry of the Tacana Volcanic Complex, Mexico-Guatemala: evidence for the last 40,000 yr of activity

Petrology and geochemistry of the Tacaná Volcanic Complex, Mexico-Guatemala: Evidence for the last 40 000 yr of activity

Article *in* Geofísica Internacional · January 2003

Source: DOAJ

CITATIONS
31

READS
240

8 authors, including:

J. C. Mora
Universidad Nacional Autónoma de México
31 PUBLICATIONS **576** CITATIONS
SEE PROFILE

J. L. Macías
Universidad Nacional Autónoma de México
195 PUBLICATIONS **3,916** CITATIONS
SEE PROFILE

Jose Luis Arce
Universidad Nacional Autónoma de México
99 PUBLICATIONS **1,131** CITATIONS
SEE PROFILE

Juan Manuel Espindola
Universidad Nacional Autónoma de México
86 PUBLICATIONS **1,361** CITATIONS
SEE PROFILE

geofísica internacional

Geofísica Internacional
Universidad Nacional Autónoma de México
secedit@tonatiuh.igeofcu.unam.mx
ISSN (Versión impresa): 0016-7169
MÉXICO

2004
J. C. Mora / J. L. Macías / A. García Palomo / J. L. Arce / J. M. Espíndola / P. Manetti / O. Vaselli / J. M. Sánchez
PETROLOGY AND GEOCHEMISTRY OF THE TACANÁ VOLCANIC COMPLEX, MEXICO-GUATEMALA: EVIDENCE FOR THE LAST 40 000 YR OF ACTIVITY
Geofísica Internacional, july-september, año/vol. 43, número 003
Universidad Nacional Autónoma de México
Distrito Federal, México
pp. 331-359

Geofísica Internacional (2004), Vol. 43, Num. 3, pp. 331-359

Petrology and geochemistry of the Tacaná Volcanic Complex, Mexico-Guatemala: Evidence for the last 40 000 yr of activity

J. C. Mora[1,3], J. L. Macías[1], A. García-Palomo[2], J. L. Arce[2], J. M. Espíndola[1], P. Manetti[3], O. Vaselli[3] and J. M. Sánchez[4]

[1] *Instituto de Geofísica, UNAM, México D.F., Mexico*

[2] *Departamento de Geología Regional, Instituto de Geología, UNAM, México D.F., México*

[3] *Dipartimento di Scienze della Terra, Universitá degli Studi di Firenze, Firenze, Italia*

[4] *Centro Interdisciplinario de Investigaciones y Estudios sobre Medio Ambiente y Desarrollo, (CIIEMAD), IPN, México, D.F.*

Received: April 24, 2003; accepted: October 30, 2003

RESUMEN

El Complejo Volcánico Tacaná (CVT) se localiza en el límite entre México y Guatemala y descansa sobre rocas metamórficas Mesozoicas e ígneas Terciarias. El CVT consiste de tres edificios volcánicos alineados de NE a SO que son Chichuj, Tacaná y San Antonio. El volcán Chichuj se encuentra constituido principalmente por flujos de lavas de composición andesítica (59-63 wt.% SiO_2). El edificio del Tacaná está constituido por flujos de lava de composición basáltico-andesítica (56-61 wt.% SiO_2) y por domos de composición andesítica y dacítica (61-64 wt.% SiO_2). Los flancos del edificio están cubiertos por depósitos de flujos de bloques y cenizas con edades de 38 000, 28 000, y 16 000 años AP. Los flujos piroclásticos están compuestos por líticos juveniles de composición andesítica (60-63 wt.% SiO_2). El volcán San Antonio está formado por flujos de lava andesíticos y domos dacíticos (58-64 wt.% SiO_2), y por un flujo de bloques y cenizas con una edad de 1950 años AP. La relación isotópica de $^{87}Sr/^{86}Sr$ de las rocas andesíticas del CVT varía de 0.70455 a 0.70459, y la de $^{143}Nd/^{144}Nd$ varía de 0.51275 a 0.51280. Una inclusión máfica de composición basáltico-andesítica presenta una relación isotópica de $^{87}Sr/^{86}Sr$ de 0.70441 y de $^{143}Nd/^{144}Nd$ de 0.51282. Las rocas pertenecen a la serie de rocas subalcalinas y siguen la alineación típica de las rocas calci-alcalinas, con contenido medio en K_2O y anomalías negativas de Nb, Ti, y P, y enriquecimiento en Tierras Raras Ligeras típico de zonas orogénicas.

PALABRAS CLAVE: Volcanismo andesítico, estratovolcán, Complejo Volcánico Tacaná, volcanes centroamericanos.

ABSTRACT

The Tacaná Volcanic Complex (TVC) on the border of Mexico and Guatemala rises above Mesozoic metamorphic and Tertiary plutonic and volcanic rocks. The TVC consists of three volcanic edifices which, from NE-to SW, are named Chichuj, Tacaná, and San Antonio. Chichuj volcano is constituted mainly of andesitic lava flows (59-63 wt.% SiO_2). Tacaná volcano is composed of basaltic-andesite lava flows (56-61 wt.% SiO_2), and andesitic and dacitic domes (61-64 wt.% SiO_2), surrounded by fans of block-and-ash flow deposits of 38 000, 28 000, and 16 000 yr BP with andesitic juvenile clasts (60-63 wt.% SiO_2). San Antonio volcano is built of lava flows, andesitic and dacitic domes (58-64 wt.% SiO_2), and one block-and-ash flow deposit dated 1,950 yr BP. The isotope ratios of the TVC andesites varies from 0.70455 to 0.70459 $^{87}Sr/^{86}Sr$ and 0.51275 to 0.51280 $^{143}Nd/^{144}Nd$. A mafic enclave has ratios of 0.70441 for $^{87}Sr/^{86}Sr$ and 0.51282 for $^{143}Nd/^{144}Nd$. The rocks belong to the sub-alkaline suite and follow the characteristic trend of calc-alkaline rocks, with medium-K content and negative anomalies of Nb, Ti, and P, and enrichment in LREE as is typical of orogenic zones.

KEY WORDS: Andesitic volcanism, stratovolcano, Tacaná Volcanic Complex, Central American volcanoes.

1. INTRODUCTION

The Tacaná Volcanic Complex (TVC) is situated on the border between the State of Chiapas, southern Mexico, and San Marcos Department, Guatemala (Figure 1A). The TVC is the northwest volcanic complex in the Central American Volcanic Arc (CAVA), stretching over 1060 km from SE Mexico to Costa Rica. The CAVA runs parallel to the trench and consists of several active stratovolcanoes that have erupted calc-alkaline magmas beginning in the Eocene (Carr *et al*., 1982; Donnelly *et al*., 1990).

Bergeat (1894) classified the rocks from Tacaná volcano as hornblende andesite, with hyperstene and olivine. Böse (1903; 1905) reported that Tacaná volcano had been built upon a granitic basement, and that there were no major petrological variations among the volcanic rocks. Ordóñez (1905) studied the volcanic rocks collected by Böse (1905) and classified them as andesites with trachytic texture composed of feldspars, Fe-Ti oxides, and augite. The precise location of the samples collected by Bergeat (1894) and Böse (1905) is unknown. De la Cruz and Hernández (1985) produced the first geological map of Tacaná: These authors con-

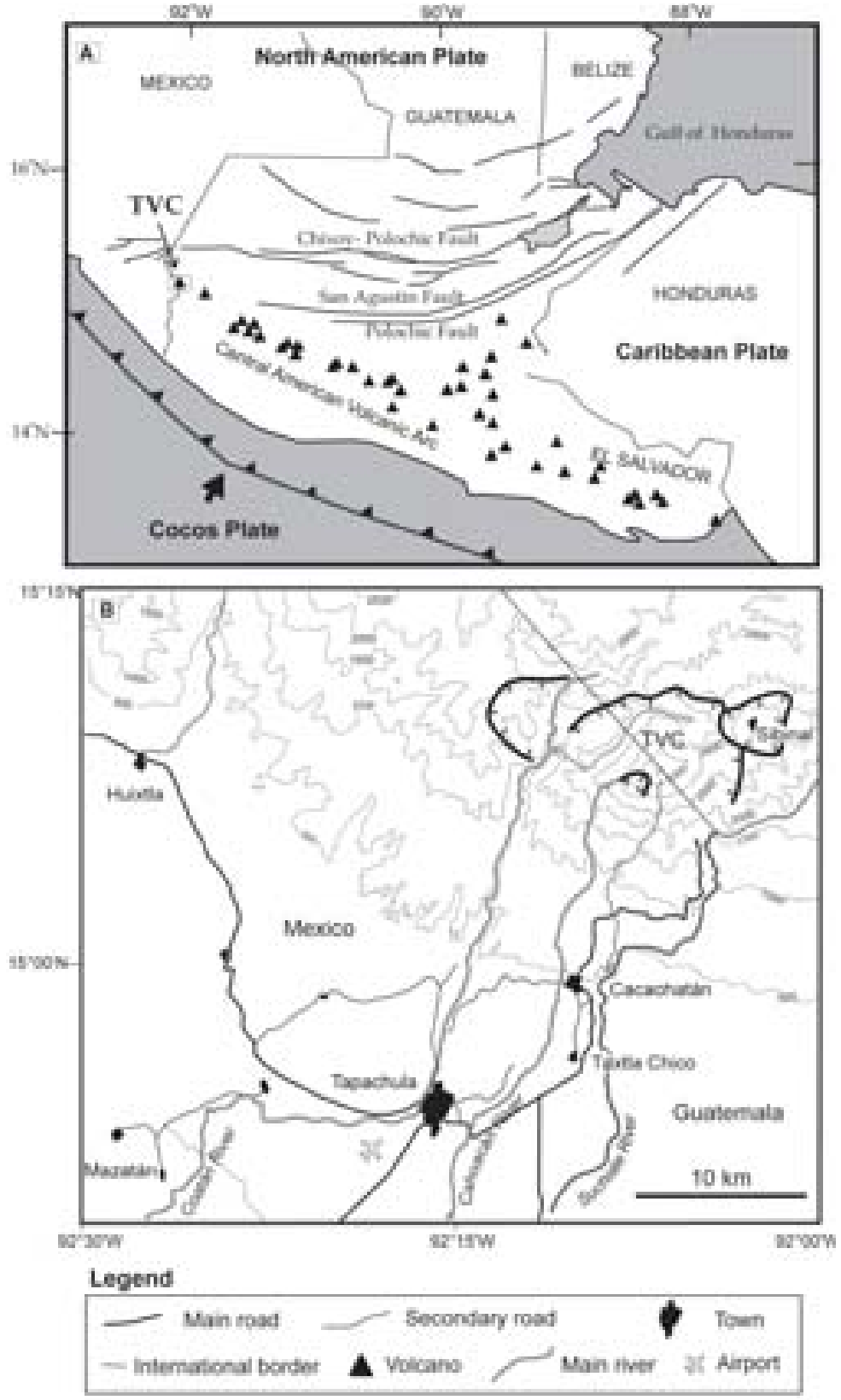

Fig. 1. A) The Tacaná Volcanic Complex (TVC) on the Guatemala-Mexico border location and tectonic setting. B) Main roads and towns surrounding the Tacaná Volcanic Complex.

sidered that Tacaná was resting on a basement constituted by metamorphic, intrusive and volcanic rocks of Paleozoic and Mesozoic age. They described lavas of andesitic and dacitic composition, with porphyritic microcrystalline textures with hornblende-augite, and hornblende-biotite, respectively.

De Cserna *et al*. (1988) concluded that Tacaná rocks are andesites of hyperstene, augite and hornblende, with xenoliths of the same mineral composition of the host rock, only finer grained and slightly mafic.

Mercado and Rose (1992) described the volcanic rocks as two pyroxene andesitic lavas with porphyritic texture containing plagioclase, pyroxene, olivine, hornblende, and quartz. Mercado and Rose (1992) presented the earliest chemical analysis of the lavas and described them as K-medium qz-normative calc-alkaline andesites.

Macías *et al*. (2000) proposed that Tacaná volcano was rather a volcanic complex composed of three volcanic edifices, namely Chichuj, Tacaná, and San Antonio (Figure 2). They identified two pyroxene andesites, with signs of disequilibrium in the mineral assemblage, and basaltic-andesitic inclusions (53.86 wt.% SiO_2). They suggest that these features were related to a magma mixing event that triggered a Peléan eruption of San Antonio Volcano in 1950 yr B.P. Mora (2001) described in detail the petrographic features and chemistry of the lava flows, the juvenile blocks from the block-and-ash-flow deposits, and the domes, all of which are dominated by a general assemblage of plagioclase, hornblende, augite, and enstatite.

We present a systematic study of the volcano in terms of its structural setting, stratigraphy, chemistry and hazard zonation. A population of about 80 000 inhabitants presently lives within 14 km of the volcano summit (Figure 1B). The nearby city of Tapachula with about 250 000 inhabitants could be affected by an eruption. We provide a general stratigraphic and geochemical framework of the complex. The main purpose is to present an overview of the petrological and geochemical characteristics of the volcano, combined with analyses of the available stratigraphic data. Finally present a model for the general evolution of the magma system and we propose some possible mechanisms of magma ascent.

2. ANALYTICAL METHODS

Sixty samples representing known deposits of the TVC including lava flows, domes, juvenile clasts and mafic enclaves from block-and-ash-flow deposits were analyzed. The chemical analysis of SiO_2, Al_2O_3, TiO_2, FeO, MnO, CaO, K_2O and P_2O_3 and trace elements (Rb, Sr, Ba, Pb, Th, Zr, Nb, La, Ce, Nd, Y, Ni, Co, Cr, Cu, and Zn) was performed by X-ray fluorescence using a PHILLIPS PW 1480 spectometer of dispersive wavelength at the Universitá degli studi di Firenze, Italia. The data were corrected for matrix effects using the absorption coefficients of mass calculated by De Vries and Jenkins (1971). The analytical accuracy is better than 5% for Rb, Sr, Ba, Zr, Nd, Ni, Co, Cr, Zn e Cu; 10% for Nb, La, Ce and Y, and 15% for Pb. Concentrations of Fe_2O_3, MgO, and Na_2O were obtained by wet chemical analyses; of MgO and Na_2O through atomic absorption spectra; Fe_2O_3 by titration using potassium dichromate ($K_2Cr_2O_7$; 0.07N), and as indicator difenilamine sulfide in H_2SO_4, after Shapiro and Brannock (1962). The amount of lost on ignition (LOI) was obtained by accounting for the mass loss during the escape of volatile components.

Concentrations of Rare Earth Elements (REE) and U, Ta, Hf, Sc, Cs, and Tb were analyzed by Inductively Coupled Plasma Mass Spectrometry (ICP-MS) and by instrumental neutron activation analysis (INAA) (Ba, Cr, Cu, Ni, Sr, Ta, V, Y, Zn, and Zr < 1 ppm; Cs, Hf, Tb, U and Th = 0.5 ppm; Rb, 20 ppm; Sm, Eu and Yb = 0.1 ppm; detection limits) at Activation Laboratories, Ancaster, Canada. Isotopic ratios $^{86}Sr/^{87}Sr$ and $^{143}Nd/^{144}Nd$ were obtained for seven representative andesitic samples from pyroclastic-flow-deposits from Tacaná, San Antonio and Chichuc volcanoes, and basaltic-andesites of the Mixcun deposit at San Antonio Volcano (SAV), at the Geochemical Isotope Laboratory (LUGIS) at Universidad Nacional Autónoma de México (UNAM).

Mineral and glass analyses were performed on the JEOL JXA-8600 electron microprobe at CNR-Università degli studi di Firenze under the following conditions: acceleration potential = 15 kV; beam current = 15 nA; and counting time 15-20 s. Glass analyses were conducted with a defocused beam 10-15 μm in diameter; for mineral analyses a focused beam was used. The data were corrected for matrix effects after method of Bence and Albee (1968). Modal abundances were determined by counting between 900 and 1000 points, consisting of phenocrysts, microphenocrysts, and groundmass (glass + microlites) using a SWIFT MODEL-F point counter adapted to a petrographic OLYMPUS-BX60 microscope.

3. TECTONIC SETTING

The Tacaná Volcanic Complex rises on the northwestern tip of the Central American Volcanic Arc (CAVA). The origin of the CAVA is related to the subduction of the Cocos plate beneath the Caribbean plate. These plates along with the North-American plate create a complicated triple point junction in the region (Guzmán-Speziale *et al*., 1989; Figure 1A). The CAVA is 1060 km long and lies about 160 to

175 km landward from the trench. It runs parallel to the coast along the Pacific ocean, from Costa Rica to the Mexico-Guatemala border until the Chixoy Polochic Fault (White, 1991). The CAVA is seismically and tectonically active; some of its active volcanoes include Arenal in Costa Rica, Cerro Negro in Nicaragua, Santa María in Guatemala, and the TVC in México. The TVC is influenced by two important tectonic features: 1) to the north the Motozintla Fault Zone, an active left strike-slip fault related to the Motagua-Polochic Transform System, which is at the border between the North America and the Caribbean plates, and 2) to the south, the subduction of the Cocos plate beneath the North America-Caribbean plates to which it is associated (Figure 1A).

Locally, the TVC is built upon metamorphic and granites of probable Mesozoic age, and granodiorites and diorites of the Chiapas Batholith of early Miocene age (20 ± 1 Ma; Mujica, 1987). The Tertiary sequence is composed of a green welded ignimbrite, and a series of indurated block-and-ash flow deposits (Macías *et al*., 2000). These rocks are transected by three important fault systems: (1) an older NW-SE fracture-fault system that affects Mesozoic and Tertiary rocks located in the western part of the complex, (2) a NE-SW oriented fault system that runs parallel to the emplacement of the TVC, and (3) a younger N-S fault system that transects the above fault systems, and that may play an important role in the activity of the volcano (Figure 1A).

4. GEOLOGY OF THE TACANÁ VOLCANIC COMPLEX (TVC)

The morphological features of the TVC consist of three NE-SW aligned volcanoes being from oldest to the youngest (Figure 2): Chichuj (3800 masl), Tacaná (4060 masl), and San Antonio (3700 masl). Only Tacaná is historically active, but diffuse fumarolic activity is present on San Antonio volcano.

4.1. Chichuj volcano (CHV)

CHV is an old, dissected, and elongated structure with its major axis aligned roughly N-S. To the E it rests discordantly on top of early Miocene rocks, whereas to the W it is bounded by two long vertical, N-S oriented, fault scarps up to 15 m high. These scarps are older collapse structures of the volcano, and they separate CHV from younger pyroclastic flow deposits from Tacaná volcano (Figure 2).

There are conspicuous lava flows in the summit area, and there are some vertical cliffs on the southern flank. A debris avalanche deposit at the base of Muxbal gully is related to Chichuj volcano (site 14). This pink massive unit contains yellow to orange hydrothermally altered zones and meter sized jigsaw blocks in a shattered matrix of coarse grained ash (Figure 3). The deposit underlies a 2 m sequence of fluviatile deposits and 10 m of light-gray block-and-ash flow deposits from Tacaná volcano, dated 28 000 yr BP. A pumice-rich pyroclastic flow deposit from Tacaná volcano covers the eastern and southeastern flanks. These flows appear in small outcrops at the summit, in the river walls (Site 91; Figure 2). A charcoal sample in this deposit yielded an age of 6910 ± 95 yr BP (Table 1).

4.2 Tacaná volcano (TV)

The summit of Tacaná (TV) has a 600-m wide crater open to the NW. Inside the crater there is a 90 m high central dome formed by three lobes. The edifice consists of lava flows and domes and its apron is made of fans of pyroclastic flow and lahar deposits (Figure 3).

The pyroclastic deposits are covered by paleosoils or by two thin ash layers from fallout of the 1902 eruption of Santa María volcano (Rose, 1972a,b). The deposits of TV rest discordantly over the Tertiary substratum.

The block-and-ash flow consists of gray dense andesitic blocks (70-80 vol.%) and minor red altered andesites embedded in an ash matrix with crystals of plagioclase, pyroxene, and angular dark-brown glass shards (Figure 3). Espíndola *et al*. (1989) described a 40 000 yr BP block-and-ash-flow deposit at La Trinidad village, on the road between Cacaohatán and Unión Juárez, south of Tacaná volcano (Table 1). Espíndola *et al*. (1993) dated another sample of the same deposit at 38 630 +5100/-3100 yr BP. They found a younger block-and-ash-flow deposit in the vicinity of Monte Perla village; a charred log sample from this unit yielded an age of >30 845 yr BP (Table 1). This deposit correlates with a block-and-ash flow exposed at site 14, in the Muxbal gully, where disseminated charcoal inside the deposit yielded an age of 28 540 ± 260 yr BP (Table 1). Multiple block-and-ash flow lobes cover the northern flanks of the volcano. At site 52, a 4m thick block and-ash-flow deposit composed of four units and two thin surge horizons 4cm each, contained disseminated charcoal within the basal unit, yielding an age of 16 350 ± 50 yr BP (Table 1).

4.3. San Antonio volcano (SAV)

SAV is the southwestern and youngest structure of the TVC. It consists of block and-ash-flow deposits, small summit lava flows, and a central summit dome (Figure 3). Macías *et al*. (2000) interpreted a block-and-ash flow (Mixcun deposit), dated at 1950 yr BP, as product of a Peléan-style eruption. This eruption destroyed the SW flank of San Antonio volcano and produced a pyroclastic flow that traveled 14 km

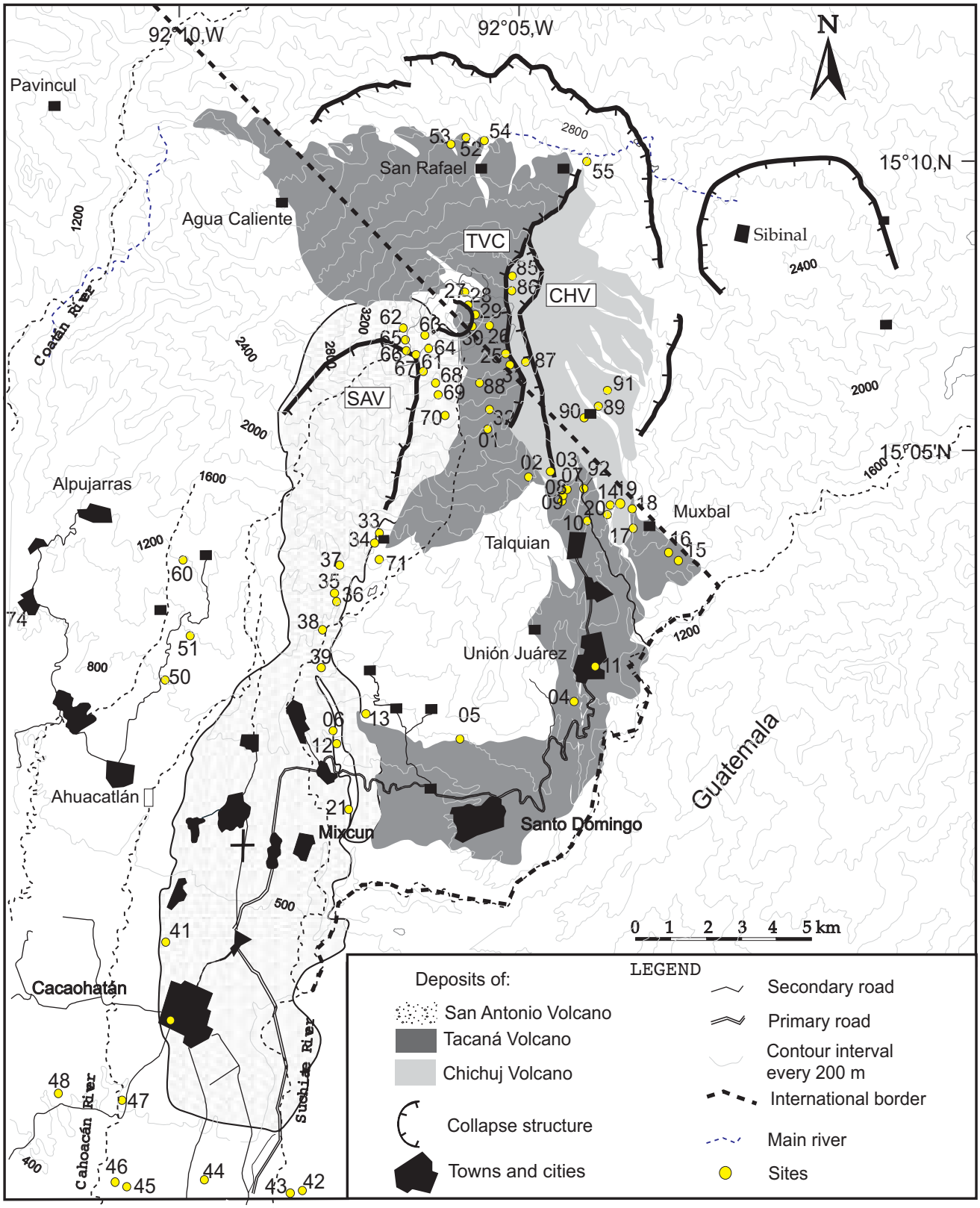

Fig. 2. Location of studied sites of the TVC. SAV, San Antonio volcano; TV, Tacaná volcano; CHV Chichuj volcano.

Table 1

Summary of radiocarbon dates of the Tacaná Volcanic Complex after Macías *et al.* (2000). 1 = ^{14}C samples analyzed at the US Geological Survey Laboratory by J. McGeehin, and 2 = ^{14}C samples analyzed at Isotope Geochemstry Laboratory of the University of Arizona by A.Long and C. Eastoe. The asterisk (*) stands for samples analyzed by the AMS method. 1) Espíndola *et al.* (1989), 2) Espíndola *et al.* (1993), 3) Macías *et al.* (2000), and 4) This work

Sample Number	LOCATION North-West		Sample Type	Conventional Age	Calibrated Age AD	Calibrated Age Range ± 1σ	Obervations	Reference
TRINIDAD	15°02'12''	92°06'51''	Charcoal	40,000			Block-and-ash flow deposit at La Trinidad	1
93TRI	15°02'12''	92°06'51''	Charcoal	38,630 +5100/-3100			Block-and-ash flow deposit at La Trinidad	2
9332	15°02'34''	92°05'11''	Charcoal	>30,845			Block-and-ash flow deposit at Monte Perla	2
9714	15°05'03''	92°04'35''	Charcoal	28,540 ± 260			Block-and-ash flow deposit at Muxbal	4
9752	15°09'29''	92°06'47''	Charcoal	16,350 ± 50			Block-and-ash flow deposit, San Marcos Department, Guatemala	4
37B[1*]	15°03'25"	92°08'42"	Charcoal	10,960 ± 50	BC 11035 12984	BC 11,169-10,948 11,205-10,879 10,778-10,707	Ash flow deposit	3
37C[1*]	15°03'25"	92°08'42"	Charcoal	9,960 ± 50	BC 9,385, 9,372, 9,349, 9,320, 9,313	BC 9,599-9,557 9,460-9,439 9,394-9,306 9,297-9,292	Ash flow deposit	3
9891	15°06'30"	92°04'40"	Charcoal	6,910 +/- 95	BC 5724	BC 5844-5664 5957-5590	Pumice flow deposit	4
9730			Charcoal	5,860±125	BC 4762, 4738, 4738 4727	BC 4900-4878 4850-4547	Pumice fall/flow deposit	
9731			Charcoal	2,905±75	BC 1110, 1050	BC 1251-1248 1206-986 957-943	Block-and-ash flow deposit	
65a[2]	15°07'28''	92°07'09''	Paleosol	2,015 ± 45			Paleosol on top of San Antonio Volcano	3
38[2]	15°07'28''	92°07'09''	Charcoal	2,370 +280/-203	BC 401	BC 799-165	MFD	3
65c[1*]	15°07'28''	92°07'09''	Charcoal	1,980 ± 40	AD 25, 43, 47	BC 2-AD 76 BC 46- AD 121	Charcoal in surge deposit on top of San Antonio Volcano	3
37d[1*]			Charcoal	1,950 ± 50	AD 34, 36, 61	AD 2-187 AD 101-123	MFD	3
12[1*]			Charcoal	1,935 ± 105	AD 72	BC 43-6 BC 5-AD 183	MFD	3
21[1*]	15°01'12''	92°08'19''	Charcoal	1,825 ± 140	AD 219	AD 30-40 AD 51-385	MFD	3
65b	15°07'28''	92°07'09''	Charcoal	600 ± 50	AD 1327, 1346, 1393	AD 1300-1372 1378-1406	Charcoal in paleosol	3

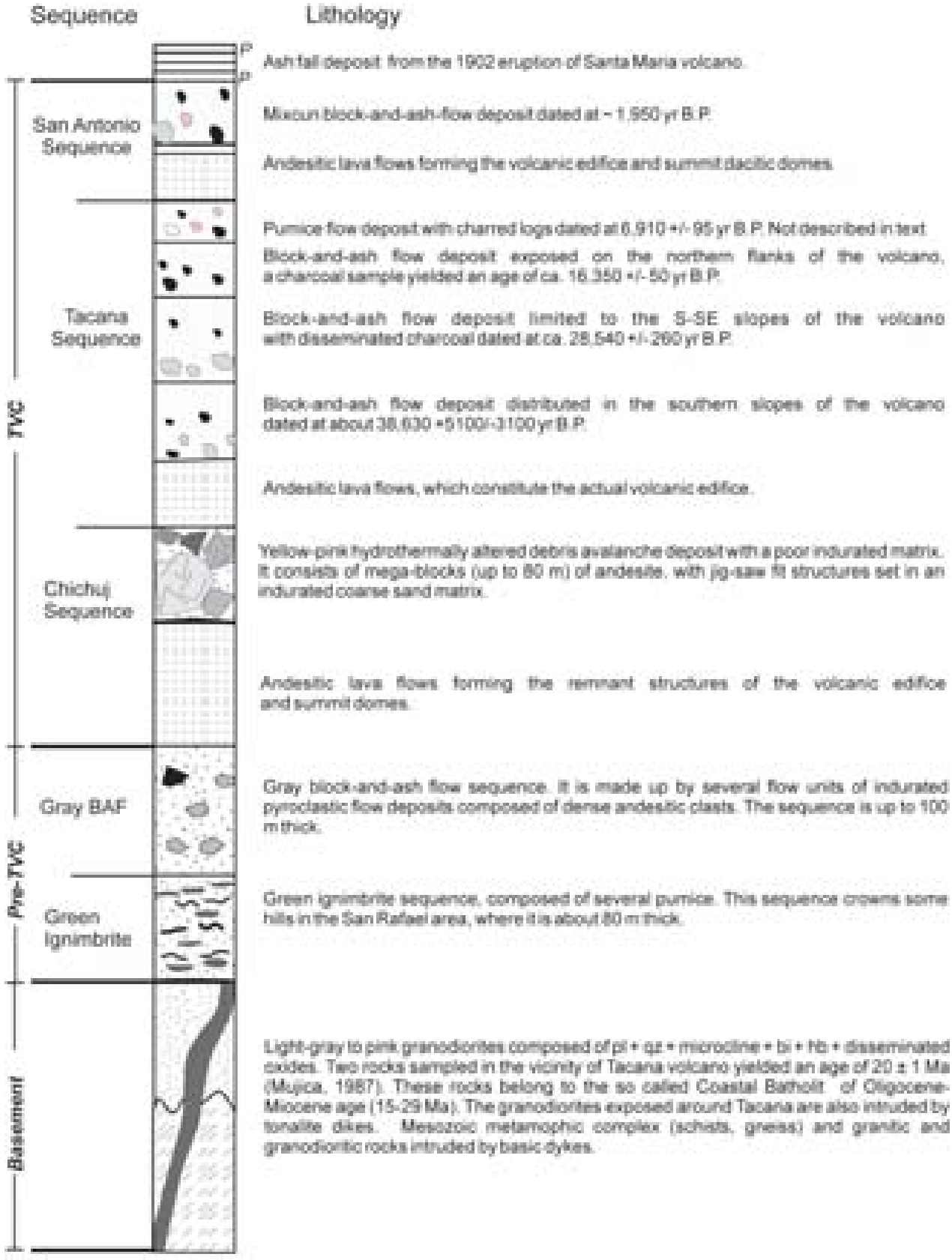

Fig. 3. Composite stratigraphic column of the Tacaná Volcanic Complex.

downstream, confined between the Cahoacán and Mixcun rivers. Macías *et al*. (2000) calculated an area of ~25 km^2 and a volume of 0.12 km^3 assuming a 5 m average thickness.

5. PETROGRAPHY AND MINERAL CHEMISTRY

Sixty samples of rocks belonging to the three volcanoes of the TVC were analyzed under the petrographic microscope. Only sixteen samples were analyzed by electron microprobe.

5.1 Chichuj volcano

Five samples of lava flows from Chichuj volcano were analyzed. The andesites of the summit are porphyritic (35% crystals) with phenocrysts and microphenocrysts of plagioclase (6.2-4.4 vol.%), clino and orthopyroxene (2.5-1.5, 1.0-0.6 vol.%), hornblende (1.1-1.0 vol.%), and Fe-Ti oxides (Table 2).

Plagioclase is the predominant mineral phase. It shows subhedral-anhedral forms, sieve and cellular textures with normal, reverse, and oscillatory zoning, resorption boundaries and broken margins, whereas euhedral forms and normal zoning predominate in the microphenocrysts (Figure 4A). Plagioclase chemical composition was obtained in the core (c), internal rim (i), and external rim (r) of the phenocrysts, and core (c) in the microphenocrysts. Plagioclase varied from andesine to labradorite in composition: An_{45-65} core and An_{40-70} rim in phenocrysts, and An_{45-65} in microphenocrysts.

Phenocrysts (<4mm) and microphenocrysts of orthopyroxene and clinopyroxene coexist in the samples. They occurr as crystal clumps and as inclusions in amphiboles. All crystals have subhedral and euhedral forms; they are slightly fractured and show some sectorial and patchy zoning (Figure 4B). The clinopyroxene is augite with little chemical variation between core and rim. It ranges from En_{40-45} in the core, and En_{42-45} in the rim. The orthopyroxene is enstatite; no chemical variations were registered between core En_{62-73}, and rim En_{67-72}.

Hornblende is present as phenocrysts from 0.5 mm to 1.5 cm in size, as single crystals or in clumps with plagioclase, orthopyroxene and titanomagnetite with their characteristic cleavage, and diamond-shaped sections (Figure 4D). Hornblende is present in subhedral and euhedral forms of green color and strong pleochroism, slightly reabsorbed margins; some crystals have slight black reaction rims due to the presence of Fe-Ti oxides (Figure 4C). All are calcic amphiboles, magnesium-hornblende in the terminology of Leake *et al*. (1997). The Al_2O_3 content is low, typically between 6-8 wt.%, up to 9 wt.% in a few crystals. Small inclusions of hornblende occur in some plagioclase with cellular and sieve textures.

Table 2

Modal analyses of the main mineral phases

Volcanic structure	Sample	Mineral Texture	% Plg		% Opx		% Cpx		% Amph.		Vesc. %	Gmass. %	Total	% Cryst.	Crystals Equi.	Crystals Diseq.
			Equi.	Diseq.	Equi.	Diseq.	Equi.	Diseq.	Equi.	Diseq.						
ChV	9885	Ph	6	8	1	0	2	0	2	2	2	66	100	31	58	42
		Mph	4	2	1	0	2	0	1	0						
	9886	Ph	9	5	1	0	3	1	1	0	4	64	100	32	78	22
		Mph	7	1	1	0	2	0	1	0						
TV	9704 ljc	Ph	9	5	2	1	2	1	2	1	3	61	100	36	77	23
		Mph	9	1	0	0	1	0	2	1						
	9707ljc	Ph	9	6	2	1	3	0	2	1	3	61	100	36	72	28
		Mph	8	2	1	0	1	0	1	0						
	9701b	Ph	8	2	2	0	2	2	1	1	3	65	100	31	82	18
		Mph	8	0	2	0	1	0	1	0						
SAV	9864	Ph	4	8	1	1	0	1	1	2	5	63	100	32	52	48
		Mph	7	2	1	0	1	1	2	1						
	9721 lj	Ph	5	8	0	1	1	1	3	1	4	62	100	34	59	41
		Mph	8	2	1	0	0	0	2	1						
	9721ljv	Ph	5	8	0	1	0	0	3	1	3	65	100	32	55	45
		Mph	6	3	0	0	1	0	2	2						
	9721 ljx	Ph	2	8	0	1	1	1	2	2	12	60	100	29	42	58
		Mph	5	2	0	0	0	0	3	2						
	9320	Ph	1	4	0	1	0	1	0	1	0	35	100	65	87	13
		Mph	38	2	2	0	2	0	15	0						

Symbology. ChV, Chichuj volcano; TV, Tacana volcano; SAV, San Antonio volcano; Plg, Plagioclase; Opx, Orthopyroxene; Cpx, Clinopyroxene; Amph., Amphibole; Vesc, Vescicle; Gmass, Groundmass; Crys, Crystals; Equi, Equilibrium; Disequi., Disequilibrium; Ph, Phenocrysts (>0.3mm); Mph, Microphenocrysts (0.3-0.03mm); Microlites, crystals in the groundmass (<0.03mm).

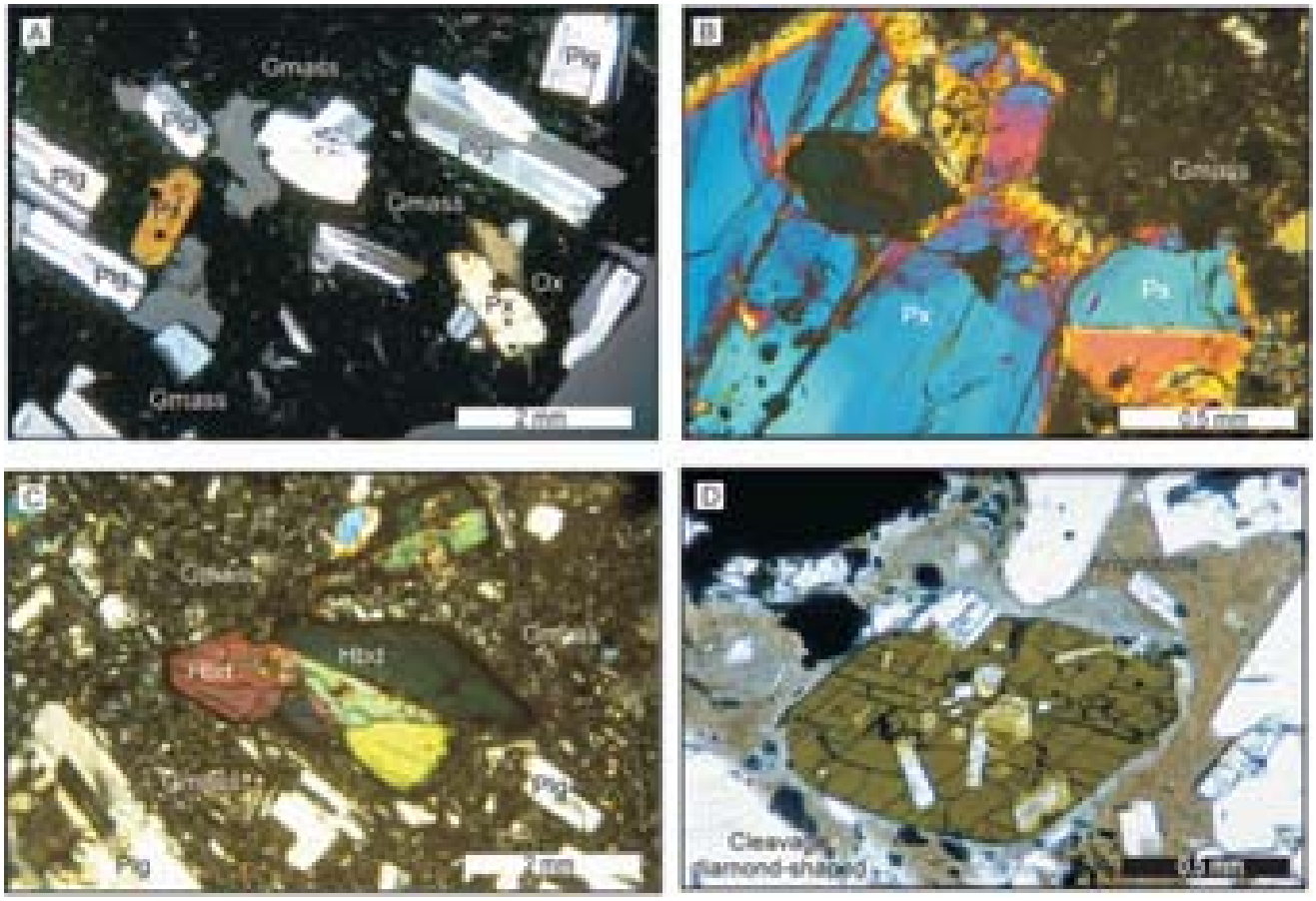

Fig. 4. Photomicrographs showing main mineral phases from lava flow samples of Chichuj volcano. A) Aligned plagioclase with subhedral-anhedral forms in a fine-grained groundmass. B) Pyroxene crystals with subhedral and euhedral forms, slight fractured, and showing sector and patchy zoning. C-D) Hornblende with characteristic cleavage, diamond-shaped sections, subhedral and euhedral forms, crystals with slight reaction rims of black color by the presence of Fe-Ti oxides.

The Fe-Ti oxides are mainly titanomagnetite and occur as individual microlites, rare microphenocrysts, inclusions in phenocrysts, and intergrowths around hornblende formed by their breakdown. Titanomagnetite has very fine-scale lamellar exsolution texture and is homogeneous in composition. The ulvöspinel (USP) and ilmenite (ILM) content in the Fe-Ti oxides was obtained by Stormer's (1983) method. The USP in titanomagnetite varies between 38.4 and 46.3%. Ilmenite is present in minor amounts, probably much less than 1% of the total Fe Ti oxide population. The ILM content in ilmenite varies from 58.9 to 67.7%. In these rocks no coexisting titanomagnetite and ilmenite was observed.

The groundmass surrounding the phenocrysts and microphenocrysts is formed by microlites of the same mineral phases and light brown glass.

5.2 Tacaná volcano

Thirty five samples of domes (4), lava flows (5), and juvenile lithics (26) from block-and-ash flow deposits of the Tacaná volcano products were analyzed (Table 3).

Lava flows were sampled at five different sites around the summit crater: these rocks have a porphyritic texture with plagioclase > hornblende > pyroxene as phenocrysts and microphenocrysts (Figure 5A). The Fe-Ti oxides appear as inclusions in phenocrysts and microlites in the groundmass. The matrix has a trachytic texture and is composed mainly of dark glass and microlites of the same mineral phases.

The three dome lobes (site 78) do not show differences in modal, and chemical composition (Figure 5B). All

Table 3

Rock total chemical composition of al igneous rocks associated at TVC

					TV					Ba
Sample	9701b	9702	9704ljc	9704ljo	9707ljc	9707ljo	9707po	9714ljc	9714ljo	9719
	Site 1	Site 2	Site 4			Site 7		Site 14		Site 19
wt.%	AC	AC	AC	AC	AC	AC	AC	AC	AC	AC
SiO_2	60.54	50.88	59.75	60.67	61.15	60.45	59.65	60.44	61.40	70.66
TiO_2	0.58	1.73	0.59	0.60	0.56	0.57	0.68	0.58	0.56	0.28
Al_2O_3	17.30	15.89	17.38	17.43	17.04	17.45	17.41	17.09	17.29	15.28
$Fe_2O_3^*$	6.22	13.99	6.36	6.03	5.89	6.15	6.19	6.20	6.08	2.73
FeO	n.m	n.m	n.m	n.m	n.m	n.m	n.m	n.m	n.m	n.m
MnO	0.11	0.23	0.11	0.11	0.11	0.11	0.11	0.11	0.11	0.07
MgO	2.30	3.71	2.44	2.42	2.28	2.24	2.44	2.32	2.33	0.67
CaO	5.54	7.87	5.68	5.52	5.68	5.85	5.63	5.64	5.73	2.83
Na_2O	3.70	3.24	3.60	3.70	3.68	3.74	3.59	3.81	3.71	4.37
K_2O	2.27	1.14	2.13	2.24	2.20	2.23	2.08	2.18	2.20	2.75
P_2O_5	0.15	0.43	0.14	0.14	0.15	0.18	0.15	0.14	0.14	0.1
LOI	1.29	0.19	1.11	1.16	0.74	0.78	1.54	1.05	0.72	0.33
Total	100	99	99	100	99	100	99	100	100	100
Trace elements ppm										
Ba	720	384	766	725	709	690	712	702	719	771
Rb	58	44	66	59	49	60	50	52	61	84
Sr	479	325	484	480	480	505	494	478	486	359
Cs	2.3	1.1	1.9	1.9	2.2	2.4	2.2	2.0	2.0	2.7
Ta	0.5	0.5	0.5	0.5	0.1	0.3	0.1	0.6	0.1	0.5
Nb	-	-	-	-	-	-	-	-	-	-
Hf	3.9	6.8	3.8	3.7	3.9	3.8	3.8	3.7	3.6	3.4
Zr	135	240	131	145	131	134	136	133	131	75
Y	17	47	18	18	17	17	18	17	18	9
Th	3.6	2.2	3.2	3.4	3.5	3.3	3.6	3.6	3.2	5.3
U	1.1	1.4	1.2	1.1	1.2	1.0	1.2	1.2	1.5	1.1
Cr	13.7	16.3	9.1	20.7	8.7	6.3	8.6	8.1	6.0	3.5
Ni	-	14	-	-	-	-	-	-	-	2
Co	13.8	33.7	14.9	13.8	15.3	13.3	15.0	14.3	13.4	5.7
Sc	10.6	43.3	11.5	11.0	10.9	10.6	11.0	10.8	10.6	2.6
V	107	298	113	112	104	107	108	108	101	32
Tb	0.4	-	0.4	0.5	0.5	0.5	0.4	0.6	0.6	-
Cu	-	104	-	-	-	-	-	-	-	8
Pb	-	2	-	-	-	-	-	-	-	17
Zn	-	137	-	-	-	-	-	-	-	57
La	16.8	15.0	16.2	16.7	16.7	16.6	16.8	16.9	16.4	17.8
Ce	34.0	41.0	31.0	34.0	34.0	34.0	34.0	34.0	34.0	35.0
Nd	15.0	28.0	16.0	16.0	16.0	14.0	15.0	15.0	17.0	15.0
Sm	3.27	6.88	3.33	3.25	3.27	3.21	3.30	3.29	3.35	3.14
Eu	0.93	1.83	0.90	0.90	0.92	0.89	0.89	0.90	0.93	0.72
Yb	1.73	4.83	1.74	1.73	1.77	1.71	1.79	1.74	1.76	0.60
Lu	0.25	0.75	0.26	0.26	0.26	0.25	0.27	0.26	0.26	0.10

Major and trace elements analyzed by Inductively Coupled Plasma Mass Spectrometry (ICP-MS) and Instrumental Neutron Activation Analysis (INAA) (<0.01% major elements; Ba, 50 ppm; Cr, Pb, Nb, V, and Rb, 2 ppm; Ni, Sc, Sr, Y, and Zr, 1 ppm; Cu, Zn and Ta, 0.5 ppm; Hf and Th, 0.2 ppm; U, 0.1 ppm; La, Ce, Nd, Sm, Tb and Yb, 0.1 ppm; Eu, 0.05 ppm, detection limits) at Activation Laboratories, Ancaster, Canada. B1, Fe2O3* is reported as total iron. AC, Activation Laboratories analyses; XRF, X-Ray Fluorescence analyses.

Table 3. Continuation

	SAV					TV				
Sample	9721ljx	9721lj	9721ljv	9721lj	9320x	9726	9727c	9727d	9733	9734
wt.%			Site 21			Site 26	Site 27		Site 33	Site 34
	AC	AC	AC	AC	AC	AC	AC	AC	XRF	XRF
SiO_2	61.98	61.77	61.24	60.36	53.86	60.98	60.52	61.51	57.93	60.21
TiO_2	0.56	0.58	0.59	0.56	0.88	0.61	0.57	0.57	0.726	0.637
Al_2O_3	16.70	16.83	16.94	16.47	18.23	17.33	16.91	16.60	18.18	17.45
$Fe_2O_3^*$	5.71	5.84	6.11	5.82	8.65	6.32	6.48	5.94	7.02	6.12
FeO	n.m	n.m	n.m	n.m	n.m	n.m	n.m	n.m	n.m	n.m
MnO	0.10	0.10	0.11	0.10	0.13	0.11	0.12	0.11	0.125	0.115
MgO	2.30	2.36	2.45	2.23	4.07	2.43	2.27	2.23	3.15	2.37
CaO	5.64	5.67	5.74	5.52	8.40	5.97	5.89	5.55	6.92	6.09
Na_2O	3.80	3.79	3.77	3.68	3.52	3.80	3.60	3.72	3.83	3.54
K_2O	2.34	2.20	2.17	2.18	1.31	2.19	2.19	2.37	1.550	2.157
P_2O_5	0.14	0.15	0.15	0.15	0.15	0.15	0.17	0.16	0.155	0.169
LOI	0.45	0.32	0.41	2.46	0.57	0.79	0.02	0.49	0.11	0.72
Total	100	100	100	100	100	101	99	99	100	100
Trace elements ppm										
Ba	699	722	677	669	490	710	664	704	619	668
Rb	61	68	58	64	29	54	64	66	40	58
Sr	481	483	490	471	568	492	491	468	580	502
Cs	2.5	2.5	2.3	2.5	1.3	2.1	1.6	2.7	-	-
Ta	0.1	0.1	0.1	0.1	0.1	0.5	0.4	0.6	-	-
Nb	-	-	-	-	-	-	-	-	4.3	5.4
Hf	3.7	3.7	3.4	3.6	2.5	3.6	3.7	3.8	-	-
Zr	122	122	126	116	95	135	127	140	133	143
Y	16	15	15	15	16	17	17	16	18	19
Th	4.1	4.2	3.8	4.3	2.0	3.3	3.7	4.5	-	-
U	1.3	1.3	1.3	1.4	0.6	1.1	1.3	1.4	-	-
Cr	15.2	15.1	12.9	11.3	34.0	6.4	4.6	7.2	4.0	3.5
Ni	-	-	-	-	-	-	-	-	0	0
Co	13.1	13.7	13.7	14.5	23.5	13.6	14.1	12.6	-	-
Sc	10.1	11.1	10.2	10.2	21.2	10.5	9.9	9.9	17.8	12.7
V	-	109	112	107	211	115	99	105	161	98
Tb	0.4	0.5	0.4	0.4	0.4	0.5	0.5	0.4	-	-
Cu	-	-	-	-	-	-	-	-	29	19
Pb	-	-	-	-	-	-	-	-	-	-
Zn	-	-	-	-	-	-	-	-	81	61
La	16.5	17.3	15.7	16.5	10.7	15.5	16.2	17.6	13.0	17.6
Ce	34.0	34.0	33.0	33.0	24.0	31.0	34.0	36.0	30.7	32.4
Nd	14.0	15.0	14.0	15.0	13.0	14.0	17.0	16.0	16.1	15.3
Sm	2.97	3.15	2.83	2.97	2.87	3.03	3.32	3.15	-	-
Eu	0.84	0.89	0.81	0.87	0.90	0.87	0.93	0.88	-	-
Yb	1.41	1.51	1.42	1.44	1.46	1.62	1.71	1.60	-	-
Lu	0.21	0.24	0.21	0.22	0.22	0.24	0.26	0.24	-	-

Isotopic analyses performed on a Finnigan MAT 262 Mass Spectrometer, LUGIS, Instituto de Geofísica, UNAM. Measured values for Sr and Nd, laboratory standards are: SRM987 = 0.710233 ± 17*, La Jolla 0.511881 ± 22*.(*) = for the last two decimals units, n = number of analyses. Analyses performed by T. Treviño, G. Solís, J. Morales, and M. Hernández. ljc = crystalline juvenile lithic; ljo = dark lithic juvenile; po = pumice; ljv = glass juvenile lithic;ljx = enclave in juvenile lithic; l = lava flow; d = dome; x = enclave; -, no missured. ChV, Chchuj volcano; TV, Tacana Volcano; SAV, San Antonio Volocano; Ba, Basement.

Table 3. Continuation

	SAV		TV							SAV
Sample	9735a	9735b	9741	9741b	9752lj	9753	9753l	9755a	9755b	9821x
wt.%	Site 35		Site 41		Site 52	Site 53		Site 55		Site 21
	XRF	XRF	XRF	XRF	XRF	XRF	XRF	XRF	XRF	XRF
SiO_2	59.53	59.81	61.73	62.39	62.68	60.13	59.15	62.86	62.52	52.30
TiO_2	0.689	0.648	0.58	0.56	0.52	0.67	0.716	0.56	0.55	0.978
Al_2O_3	17.57	18.14	17.55	17.30	17.61	18.22	17.55	16.88	17.27	18.52
$Fe_2O_3^*$	6.52	5.84	1.75	3.82	0.63	2.59	6.62	1.43	1.41	8.80
FeO	n.m	n.m	3.40	1.44	3.44	3.32	n.m	3.20	3.22	n.m
MnO	0.117	0.105	0.12	0.12	0.10	0.12	0.116	0.11	0.11	0.134
MgO	3.00	2.46	2.52	2.34	2.16	2.31	3.19	2.22	2.17	4.75
CaO	5.92	5.61	6.04	5.66	5.79	6.53	6.27	5.45	5.70	8.93
Na_2O	3.61	3.59	3.71	3.72	3.75	3.69	3.78	3.80	3.74	3.42
K_2O	1.921	1.829	2.03	2.06	2.10	1.70	1.785	2.17	2.13	1.016
P_2O_5	0.159	0.174	0.13	0.13	0.13	0.12	0.160	0.14	0.15	0.160
LOI	0.43	1.41	0.43	0.45	1.08	0.60	0.15	1.17	1.03	0.59
Total	99	100	100	100	100	100	99	100	100	100
Trace elements ppm										
Ba	837	832	734	743	756	712	681	756	748	443
Rb	53	42	59	62	65	50	44	65	65	22
Sr	511	560	505	488	486	572	583	486	527	614
Cs	-	-	-	-	-	-	-	-	-	-
Ta	-	-	-	-	-	-	-	-	-	-
Nb	5.0	5.7	4.0	3.0	4.0	5.0	4.5	5.0	4.0	3.4
Hf	-	-	-	-	-	-	-	-	-	-
Zr	139	160	125	132	134	114	126	127	132	89
Y	17	16	13	12	12	11	15	12	13	18
Th	-	-	6.0	4.0	7.0	6.0	-	5.0	6.0	-
U	-	-	-	-	-	-	-	-	-	-
Cr	20.7	9.4	40.0	35.0	53.0	13.0	9.7	7.0	2.0	36.3
Ni	0.6	0	68	27	8	-	0	-	-	5.1
Co	-	-	16.0	14.0	9.0	16.0	-	13.0	11.0	-
Sc	15.8	14.1	-	-	-	-	16.3	-	-	27.5
V	118	108	115	108	87	132	131	97	95	210
Tb	-	-	-	-	-	-	-	-	-	-
Cu	27	12	9	9	3	10	16	6	4	36
Pb	-	-	7	12	12	10	-	9	11	-
Zn	71	74	66	75	57	77	74	68	67	72
La	14.1	16.5	16.0	19.0	21.0	24.0	14.9	16.0	17.0	9.0
Ce	33.1	32.6	35.0	32.0	38.0	42.0	30.5	43.0	42.0	22.4
Nd	14.8	15.1	15.0	16.0	19.0	21.0	12.8	20.0	20.0	11.7
Sm	-	-	-	-	-	-	-	-	-	-
Eu	-	-	-	-	-	-	-	-	-	-
Yb	-	-	-	-	-	-	-	-	-	-
Lu	-	-	-	-	-	-	-	-	-	-

samples are light-gray in color with phenocrysts and microphenocrysts of plagioclase > hornblende > pyroxene and Fe-Ti oxides as inclusions in phenocrysts, and microlites (Figure 5A). The matrix is dark glass with microlites of all mineral phases (Figure 5A).

The juvenile lithics are porphyritic with phenocrysts and microphenocrysts of plagioclase (10.5-15.3 vol.%), clinopyroxene and orthopyroxene (0.6-1.2; 0.4-0.9 vol.%), and hornblende (1.2-3.6 vol.%). The Fe-Ti oxides are dispersed as microlites in the groundmass, and as inclusions in

Table 3. Continuation

	SAV		TV	SAV						TV
Sample	9821xin	9821in	9859	9860	9863	9864d	9865ab	9865p	9866	9867
wt.%	Site 21		Site 59	Site 60	Site 63	Site 64			Site 66	Site 67
	XRF	XRF	AC	XRF	XRF	XRF	XRF	XRF	XRF	XRF
SiO_2	58.58	62.20	54.12	56.12	61.76	64.41	61.32	62.43	63.74	61.90
TiO_2	0.79	0.589	1.44	0.810	0.620	0.45	0.585	0.58	0.513	0.55
Al_2O_3	17.73	16.82	14.95	18.59	17.07	17.30	16.90	16.61	17.48	17.79
$Fe_2O_3^*$	2.70	5.44	3.07	7.24	5.82	0.90	5.51	2.28	4.39	1.82
FeO	3.22	n.m	7.80	n.m	n.m	2.76	n.m	2.95	n.m	2.80
MnO	0.13	0.103	0.19	0.131	0.118	0.09	0.105	0.11	0.081	0.10
MgO	3.24	2.33	4.48	3.13	2.54	2.31	2.56	2.44	1.75	2.81
CaO	7.33	5.46	7.64	7.54	5.76	5.04	5.72	5.88	4.73	5.96
Na_2O	3.66	3.69	3.13	3.84	3.69	3.82	3.64	3.69	4.54	3.71
K_2O	1.70	2.204	1.59	1.733	2.114	2.17	2.118	2.06	2.006	2.05
P_2O_5	0.14	0.148	0.22	0.237	0.156	0.15	0.146	0.12	0.157	0.12
LOI	0.77	0.68	1.38	0.12	0.22	0.59	0.54	0.85	0.33	0.39
Total	100	100	100	99	100	100	99	100	100	100
Trace elements ppm										
Ba	627	686	579	711	686	836	717	708	823	757
Rb	45	64	45	35	59	49	60	63	46	62
Sr	551	508	550	805	509	484	492	489	671	490
Cs	-	-	4.4	-	-		-	-	-	-
Ta	-	-	1.9	-	-		-	-	-	-
Nb	8.8	5.3	5.0	4.5	5.2	3.0	5.6	4.0	4.9	4.0
Hf	-	-	4.9	-	-		-	-	-	-
Zr	129	138	123	119	135	126	138	122	147	125
Y	13	16	12	19	15	9	15	11	11	12
Th	-	-	4.3	-	-	7.0	-	9.0	-	6.0
U	-	-	-	-	-		-	-	-	-
Cr	45.0	9.7	41.2	5.3	13.9	17.0	16.1	19.0	7.5	57.0
Ni	-	0	25	0	0		1.7	1	0	12
Co	-	-	14.0	-	-	10.0	-	14.0	-	14.0
Sc	-	12.7	-	14.9	14.4		13.0	-	10.3	-
V	-	83	-	162	107	82	106	116	67	104
Tb	-	-	0.5	-	-		-	-	-	-
Cu	-	14	-	28	12		14	5	11	8
Pb	-	-	-	-	-	12	-	12	-	9
Zn	-	58	55	90	67	54	69	75	66	60
La	11.8	16.5	14.4	16.1	16.3	16	16.3	20.0	17.5	17.0
Ce	35.6	34.2	32.0	31.7	32.5	39	32.7	39.0	34.5	29.0
Nd	-	14.4	48.0	18.0	13.8	20	13.1	17.0	13.6	14.0
Sm	-	-	4.90	-	-		-	-	-	-
Eu	-	-	1.33	-	-		-	-	-	-
Yb	-	-	2.90	-	-		-	-	-	-
Lu	-	-	0.40	-	-		-	-	-	-

phenocrysts. The groundmass is composed by microlites of the main mineral phases and dark brown glass. All juvenile clasts have similar crystallinities varying from 35 to 39 vol.% (Table 2).

Plagioclase is the most abundant crystalline phase in all analyzed samples. The largest grains are 3 mm in length display complex zoning, sieve and cellular textures, whereas microphenocrysts and microlites exhibit normal and reverse zoning (Figure 5B). Plagioclase appears either as single crystals, or as glomerocrysts (<0.5 cm), or as inclusions in pyroxene and amphibole phenocrysts. Rounded to irregular

Table 3. Continuation

	SAV		TV							ChV
Sample	9870a	9870B	9871	9875	9876a	9876b	9878a	9878b	9878c	9884
wt.%	Site 70		Site 71	Site 75	Site 76			Site 78		Site 84
	XRF	XRF	XRF	XRF	AC	XRF	AC	XRF	XRF	XRF
SiO_2	61.03	55.57	59.67	56.60	57.20	60.67	63.30	62.78	62.88	62.93
TiO_2	0.605	1.244	0.661	0.729	0.73	0.591	0.53	0.551	0.53	0.561
Al_2O_3	17.23	16.21	17.74	17.98	18.67	17.22	17.15	16.88	17.44	16.87
$Fe_2O_3^*$	5.85	9.34	6.56	7.43	3.07	5.79	1.57	5.26	1.61	5.36
FeO	n.m	n.m	n.m	n.m	3.52	n.m	2.78	n.m	2.66	n.m
MnO	0.112	0.158	0.113	0.172	0.17	0.111	0.11	0.100	0.10	0.105
MgO	2.38	4.05	2.68	2.75	2.61	2.32	2.17	2.17	2.17	2.26
CaO	5.74	7.41	6.16	7.93	7.98	5.70	5.81	5.34	5.87	5.35
Na_2O	3.58	3.36	3.62	3.55	2.81	3.64	3.86	3.70	3.84	3.68
K_2O	2.135	1.368	1.829	1.482	1.50	2.058	2.24	2.316	2.18	2.323
P_2O_5	0.157	0.065	0.171	0.248	0.21	0.155	0.13	0.150	0.12	0.150
LOI	1.01	0.70	0.31	0.61	1.02	1.17	0.35	0.23	0.80	0.23
Total	100	99	100	99	99	99	100	99	100	100
Trace elements ppm										
Ba	715	460	653	723	917	710	875	729	763	729
Rb	58	40	45	37	33	53	64	67	61	67
Sr	501	358	551	765	704	519	491	500	502	501
Cs	-	-	-	-	3.0	-	5.7	-	-	-
Ta	-	-	-	-	-	-	2.7	-	-	-
Nb	5.2	4.7	5.1	5.0	6.3	5.2	8.8	5.3	8.0	5.4
Hf	-	-	-	-	4.2	-	4.1	-	-	-
Zr	149	99	135	138	128	138	148	143	146	136
Y	17	20	18	23	19	17	12	15	13	16
Th	-	-	-	-	4.7	-	4.2	-	-	-
U	-	-	-	-	1.3	-	1.8	-	-	-
Cr	5.5	38.3	5.8	4.5	17.9	6.8	19.6	8.7	17.9	9.4
Ni	0	25.4	0	0.7	45	0	-	0	-	0
Co	-	-	-	-	15.4	-	14.5	-	-	-
Sc	11.7	35.4	14.9	12.9	13.8	13.3	10.6	12.1	-	11.2
V	98	270	119	118	98	100	-	72	-	67
Tb	-	-	-	-	0.4	-	0.6	-	-	-
Cu	12	80	15	17	-	15	-	12	-	12
Pb	-	-	-	-	-	-	-	-	-	-
Zn	66	90	72	81	117	77	72	54	-	54
La	16.4	5.1	15.7	16.5	20.8	17.7	20.0	18.0	19.2	16.7
Ce	31.7	15.5	31.0	35.0	45.0	33.8	35.0	33.2	33.1	33.3
Nd	15.2	9.4	15.8	19.9	20.0	16.1	45.0	14.1	-	14.8
Sm	-	-	-	-	6.00	-	3.50	-	-	-
Eu	-	-	-	-	1.49	-	0.96	-	-	-
Yb	-	-	-	-	1.90	-	1.70	-	-	-
Lu	-	-	-	-	0.30	-	0.20	-	-	-

glass inclusions are often present within plagioclase phenocrysts. The inclusions are concentrated in crystal cores or along zones parallel to crystal margins (Figure 5A). Apatite occurs as inclusions along zones paralleling crystal margins; in some crystals they tend to be oriented tangentially to the plagioclase rims. The chemical composition of plagioclase in andesitic and dacitic rocks varies from andesine to labradorite. The anorthite content varies from 40-68% in the core, and 41-72% in the rim, showing normal, oscillatory and reverse crystal zoning.

Table 3. Continuation

					TV				
Sample	9885	9887	9889	9890	9891lj	9891p	9892a	9892b	9892c
wt.%	Site 85	Site 87	Site 89	Site 90	Site 91			Site 92	
	XRF	AC	XRF	XRF	XRF	XRF	XRF	XRF	XRF
SiO_2	62.22	58.77	59.95	62.71	61.48	60.38	62.22	62.08	60.68
TiO_2	0.56	0.69	0.61	0.54	0.568	0.51	0.56	0.59	0.64
Al_2O_3	17.65	18.74	18.56	17.84	17.39	19.82	17.16	17.47	18.25
$Fe_2O_3^*$	1.56	3.68	3.86	2.28	5.80	2.15	1.13	1.79	2.03
FeO	2.90	2.28	1.70	2.26	n.m	2.16	3.52	2.76	3.20
MnO	0.11	0.12	0.11	0.11	0.114	0.10	0.11	0.10	0.11
MgO	2.14	3.02	2.89	2.22	2.25	2.09	2.32	2.42	2.36
CaO	5.68	6.22	6.20	5.47	5.64	4.51	5.77	5.46	6.40
Na_2O	3.70	3.64	3.77	3.68	3.74	3.39	3.68	3.84	3.97
K_2O	2.18	1.85	1.87	2.30	2.078	2.11	2.29	2.24	1.87
P_2O_5	0.16	0.11	0.13	0.13	0.156	0.13	0.13	0.13	0.12
LOI	1.14	0.88	0.36	0.46	0.08	2.64	1.12	1.13	0.37
Total	100	100	100	100	99	100	100	100	100
Trace elements ppm									
Ba	773	689	716	812	780	740	779	777	708
Rb	57	55	47	58	60	43	54	50	44
Sr	487	481	512	481	520	471	489	512	560
Cs	-	2.0	-	-	-	-	-	-	-
Ta	-	1.3	-	-	-	-	-	-	-
Nb	7.8	7.4	8.2	8.2	5.2	6.6	7.6	7.9	7.9
Hf	-	3.9	-	-	-	-	-	-	-
Zr	150	131	126	145	143	152	140	135	132
Y	13	14	13	14	17	13	13	11	12
Th	-	4.0	-	-	-	-	-	-	-
U	-	2.0	-	-	-	-	-	-	-
Cr	31.8	33.5	28.3	28.3	5.0	16.2	30.1	23.1	42.2
Ni	-	70	-	-	0	-	-	-	-
Co	-	17.9	-	-	-	-	-	-	-
Sc	-	17.8	-	-	10.8	-	-	-	-
V	-	-	-	-	79	-	-	-	-
Tb	-	0.7	-	-	-	-	-	-	-
Cu	-	-	-	-	10	-	-	-	-
Pb	-	-	-	-	-	-	-	-	-
Zn	-	138	-	-	56	-	-	-	-
La	15.5	17.2	15.1	20.3	15.7	26.8	17.1	15.9	11.8
Ce	42.2	34.0	40.4	35.0	30.2	38.2	30.9	33.1	32.3
Nd	-	14.0	-	-	13.3	-	-	-	-
Sm	-	4.20	-	-	-	-	-	-	-
Eu	-	1.54	-	-	-	-	-	-	-
Yb	-	1.80	-	-	-	-	-	-	-
Lu	-	0.22	-	-	-	-	-	-	-

Fig. 5. A) Photomicrographs of porphyritic texture in sample TAC9704 (juvenile clast) with phenocrysts of plagioclase and pyroxene in a groundmass with microlites of the same constituents. B) Photograph from the northwest of the central dome at the Tacaná summit. C) Pyroxene crystal with subhedral and euhedral forms, slightly fractured, with slight sector and patchy zoning.

The hornblende always appears as phenocrysts and microphenocrysts with euhedral-subhedral forms; Fe-Ti oxides surround some hornblende crystals. The hornblende varies from dark green to slightly red, and is strongly pleochroic. Phenocrysts (<2 mm) have numerous glass and mineral inclusions distributed in the crystal. The hornblende is Mg-rich and belongs to the calcic-amphibole group (Leake *et al*., 1997).

Orthopyroxene and clinopyroxene occur as euhedral-subhedral phenocrysts (< 4 mm) and microphenocrysts, in crystal clumps and as small inclusions in hornblende. All crystals are slightly fractured and sector zoning (Figure 5C).

Clinopyroxene is mainly augite. In andesitic and dacitic rocks the enstatite content in phenocrysts and microphenocrysts varies from En_{39-43} in the core to En_{40-43} in the rim, whereas microlites in the groundmass are En_{40}. Minor variations were registered between core and rim in phenocrysts, where normal zoning was predominant.

Orthopyroxene crystals fall mainly in the enstatite field with a homogeneous composition. In andesites and dacites the enstatite content varies from En_{63-70} in the core, to En_{65-68} in the rim, and microlites registered En_{64-67}.

The Fe-Ti oxides are predominantly titanomagnetite with little ilmenite. Titanomagnetite is present as microlites and inclusions in phenocrysts, and rarely as microphenocrysts. Sometimes it is found surrounding hornblende as a reaction border. Titanomagnetite has ulvöspinel (USP) content from 17.5 to 31.8%. Ilmenite has ILM content between 65.5 and 68.5%.

The groundmass (61-65 vol.%) is composed by microlites and honey colored glass (Table 2).

5.3 San Antonio volcano

Eighteen samples of the summit dome (3), lava flow (4), juvenile lithics (8), and mafic enclaves (3) hosted by

juvenile lithics of SAV were studied (Table 3). The dome, lava flow and juvenile lithics have a porphyritic texture, with phenocrysts (<4 mm) and microphenocrysts of plagioclase (10-13 vol.%), hornblende (3.2-4.4 vol.%), and pyroxene (0.6-1.6 vol.%). All crystals are surrounded by a groundmass of microlites of the same mineral phases plus Fe-Ti oxides, and dark brown glass.

The mafic enclaves have elongated and ellipsoidal forms, with glass between the mineral phases, and chilled margins in contact with the host rock. They are dark gray to black basaltic-andesite (site 21). These rocks have intersertal texture with brown glass between microphenocrysts of plagioclase (37.6 vol.%), hornblende (14 vol.%), pyroxene (2 vol.%), and olivine (< 1 vol.%). The enclaves have phenocrysts of plagioclase (3.6 vol.%), hornblende (1.3 vol.%), and pyroxene (0.5 vol.%). In general the enclaves have ~65 vol.% of crystals (Figure 6G-H).

Plagioclase is the most abundant mineral phase in juvenile blocks of andesitic and dacitic composition. It is present as phenocrysts, microphenocrysts and microlites of plagioclase with euhedral and subhedral forms, and numerous glass inclusions (Figure 6C). These inclusions are concentrated in the core, rim, or aligned following growing planes, or scattered in the crystal (Figure 6C). Plagioclase has margins and cores, as well as reverse, normal and oscillatory zoning (Figure 6D). Plagioclase in the andesites varies from andesine to labradorite with an anorthite content of An_{45-73} in the core, and An_{40-84} in the rim. In the dacites the anorthite content varies from An_{45-69} in the core to An_{80} in the rim.

Plagioclase in mafic enclaves is predominantly present as microphenocrysts of euhedral tabular forms aligned parallelly or intercrossed. Only a few plagioclase phenocrysts show sieve and cellular textures (Figure 6H). It varies in composition from bytownite to labradorite, and some crystals fall in the andesine field. In the andesitic and dacitic rocks it varies from labadorite to andesine, and minor crystals are bytownite. The anorthite content in the mafic enclave plagioclase varies from An_{49-88} in the core to An_{48-84} in the rim; in the andesitic rocks it varies from An_{45-73} in the core to An_{40-84} in the rim, whereas plagioclase in the dacitic rocks have An_{45-69} in the core and An_{80} in the rim.

Hornblende is the most abundant mineral phase after plagioclase. In andesitic and dacitic rocks it appears as phenocrysts, microphenocrysts, and microlites with euhedral and subhedral forms. The phenocrysts have numerous glass and mineral inclusions. Black reaction rims occur around phenocrysts due to the presence of Fe-Ti oxides (Figure 6C-D). Few crystals have reabsorbed zones in the core or rim that is occupied by the groundmass (Figure 6D). Reaction rims were observed following exfoliation planes, and in fracture planes within crystals as well.

Hornblende in the mafic enclaves appears as microphenocrysts of elongated, rounded and tabular forms, occupying spaces between plagioclase and pyroxene crystals (Figure 6G). The phenocrysts have subhedral forms surrounded by reaction rims composed by small pyroxene crystals (Figure 6G). Amphibole has a calcic amphibole composition, varying from mg-hornblende in the juvenile clasts, to mg-hastingsite in the mafic enclaves.

The pyroxene (clinopyroxene and orthopyroxene) has euhedral and subhedral forms with some dilution in the margins and within the crystal. Numerous glass and mineral plagioclase and Fe-Ti oxides inclusions are present inside the crystal (Figure 6B-F). The pyroxene occurs as both individual crystals and clots with plagioclase and Fe-Ti oxides (Figure 6F). Chemical analyses from core and rim of pyroxene crystals do not show significative differences; they show mainly normal zoning. The clinopyroxene falls in the augite field, the enstatite content in the pyroxenes of andesitic rocks varies from En_{40-45} (core), to En_{42-44} (rim), whereas in the dacitic rocks it does not show major variations (En_{41-42}). The orthopyroxene falls in the enstatite field, with an enstatite content of En_{62-73} (core), and En_{67-72} (rim), in the andesites. In dacites it varies from En_{66-71} to En_{70}, in the core and rim, respectively.

Pyroxenes in the mafic enclaves are predominantly microphenocrysts with minor proportions of phenocrysts. Microphenocrysts have long subhedral forms parallel to the plagioclase and hornblende crystals; some microphenocrysts of pyroxene occupy spaces between hornblende and plagioclase crystals. The clinopyroxene falls in the boundary between diopside and augite, with an enstatite content varying from En_{39-41} (core), to En_{41-42} (rim); whereas orthopyroxene varies from En_{64-67} to En_{68} in the core and rim, respectively.

The Fe-Ti oxides are titanomagnetite and ilmenite these are microlites dispersed in the groundmass and as inclusions in the phenocrysts.

Olivine occurs as rounded to anhedral microphenocrysts, also as reacted phenocrysts. Olivines contain only occasional titanomagnetite and glass inclusions. It is present only in the mafic enclaves (site 21), and rare crystal fragments were observed in the andesite rocks too. Olivine has a homogeneous chemical composition varying around Fo_{76-79}.

6. CHEMISTRY OF THE TVC

Mercado and Rose (1992) were the first authors to publish chemical analyses of rocks from Tacaná volcano. They

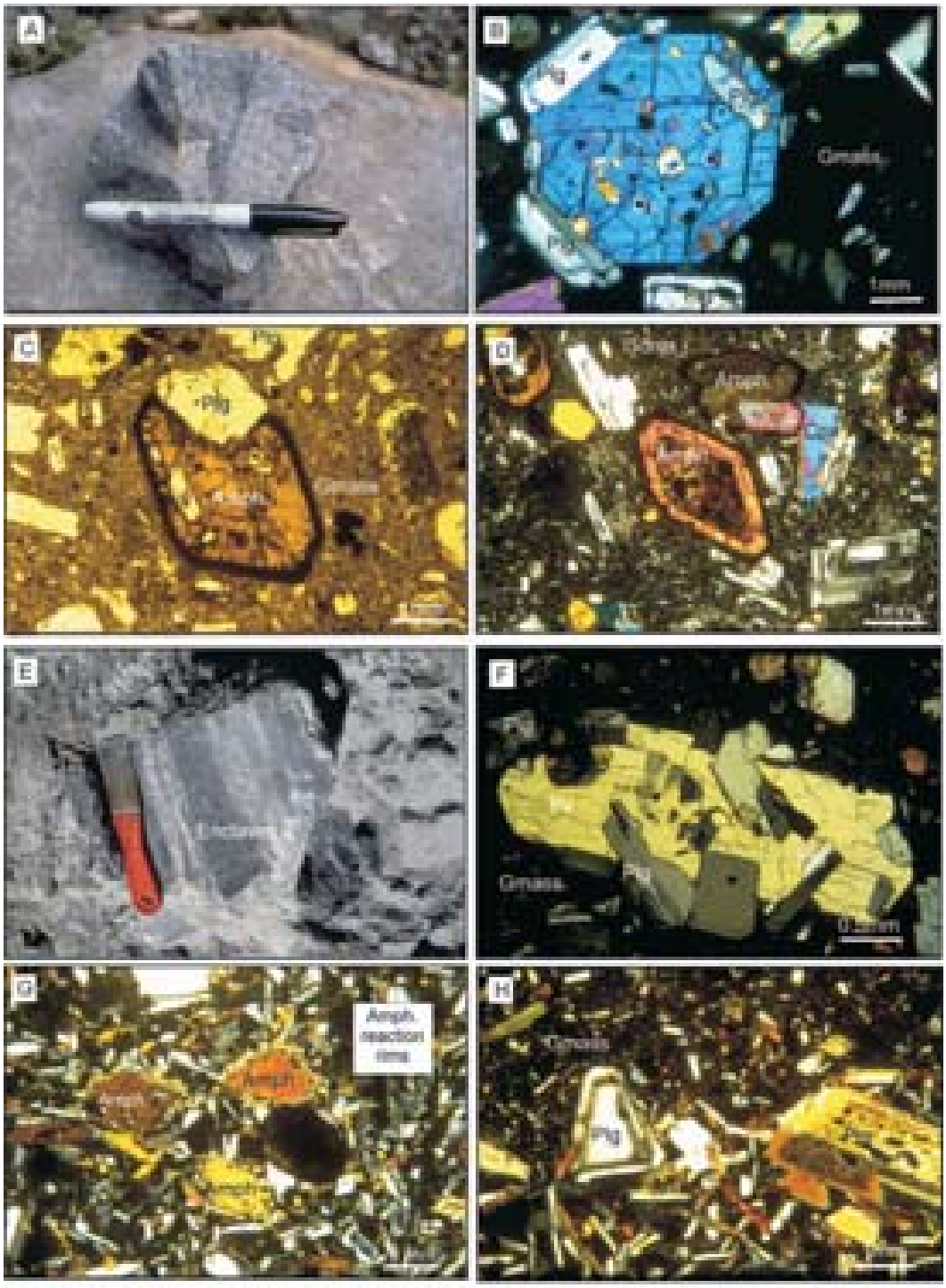

Fig. 6. A) Photograph of a gray juvenile lithic with cooling fractures from Mixcun deposit at site 21. B) Photomicrograph of a euhedral pyroxene phenocryst surrounded by euhedral plagioclase in andesitic and dacitic rocks. C-D) Photomicrographs of hornblende phenocrysts in andesitic and dacitic rocks with euhedral forms and reaction rims blackened by the presence of Fe-Ti oxides. D) Photomicrograph of a hornblende crystal with reabsorbed core occupied by groundmass. E) Photograph of a banded enclave hosted by andesitic juvenile clast at site 21 (Mixcun deposit). F) Photomicrographs of an orthopyroxene phenocryst with numerous glass and mineral inclusions. G) Microphotograph of a mafic enclave composed mainly by microphenocrysts of plagioclase, amphibole, and pyroxene with an interstitial texture with few phenocrysts of plagioclase, amphibole and pyroxene. There are three amphibole phenocrysts in the center with pyroxene reaction rims. H) Photomicrographs of a mafic enclave whereas the plagioclase appears predominantly as microphenocrysts of euhedral tabular forms parallell aligned or intercrossed. Few plagioclase phenocrysts have sieve and cellular textures.

analyzed 16 samples of lava, ash, and lithics from different deposits that yielded SiO_2 contents between 58 and 64 wt.%. Macías *et al*. (2000) and Mora (2001) initiated a more systematic study of the rocks associated with the TVC. They recognized a far larger variation in the composition, from 50 to 64 wt.% SiO_2, and reported mafic intrusions in granites and mafic enclaves hosted in andesitic rocks (Table 3).

6.1 Rock classification

Major and trace element analyses of 60 samples from TVC were obtained in this work. The TVC rocks have been classified on the basis of whole-rock composition in the silica versus alkali (Na_2O+K_2O) TAS diagram (Le Bas *et al.,* 1986), these rocks plot in the fields of basaltic-andesite (mafic enclaves), andesite (juvenile clasts and lava flows), and dacite (lava flows and domes) (Figure 7A). All rocks belong to the sub-alkaline suite and are calc-alkaline (Irvine and Baragar, 1971). In the K_2O vs. SiO_2 diagram for calc-alkaline suites (Gill, 1981) they plot in the medium-K field (Figure 7B). The rocks have low TiO_2 (<1 vol.%) and high Al_2O_3 (14-19 wt.%) contents, typical of orogenic volcanic rocks (Figure 7C, E).

6.2 Major elements

TVC has generated a homogeneous compositional range of andesitic and dacitic rocks. The most basic compositions known are basaltic-andesites from the TV and SAV. Figure (7C-H) shows Harker-type diagrams of silica vs. major elements using the silica as differentiation index. There are no major differences between samples of the three volcanic edifices (CHV, TV, and SAV). TiO_2, Al_2O_3, MgO, and CaO show a negative correlation with increasing SiO_2 (Figure 7), whereas K_2O follow a positive correlation, and Na_2O and P_2O_5 remains constant (Figure 7F,H). Volcanic products of CHV have an andesitic homogeneous composition with a variation of ~4% in SiO_2 content; whereas in the TV rocks, (juvenile clasts, and domes) it varies about 3%, from 60.49 to 63.52 wt.%; and in the SAV rocks (lavas, domes and juvenile clasts) the variation is about 6%, from 58.17 to 64.17 wt.%; the mafic enclaves vary from 52.82 to 54.29 wt.%. There is an apparent compositional gap between 54.29 to 58.17 wt.% in silica between the mafic enclaves and the lavas, domes and juvenile clasts of SAV rocks (Figure 7).

6.3 Trace elements

Trace element values in the analyzed rocks are plotted versus silica (Figure 8). As with the major elements, no major difference exists between the three volcanic edifices. Nevertheless, some small differences can be observed. Ba, Rb, La, and Ce are positively correlated with SiO_2, whereas Sr, V, Co, and Sc decrease with SiO_2. Hf, Zr, Y, Eu, Nd, Yb, and Lu are relatively constant with silica. The low Ni and Cr concentrations of all andesitic and dacitic rocks suggest that they were fractionated in the magma chamber.

The trace element pattern normalized to the concentrations of the primordial mantle (Wood, 1979) is shown in Figure 9. The pattern of rare earth elements normalized to their chondritic abundances (Nakamura, 1974) shows enrichment in light rare earth elements (LREE), and depletion in heavy rare earth elements (HREE). These patterns are typical of orogenic calc-alkaline suites (Gill, 1981) with europium anomaly, with enrichment in LILE and with negative anomalies of Nb (Figure no showed in this study). Rare earth elements for the mafic enclaves show a similar trend as the andesite rocks but with minor concentration of rare earth elements.

6.4 Sr and Nd isotopes

Representative isotopic ratios for samples spanning the compositional range of Tacaná magmas are listed in Table 4. The isotopic ratios $^{87}Sr/^{86}Sr$ and $^{143}Nd/^{144}Nd$ were obtained from one andesite sample and one dacite sample from every volcano, plus one mafic enclave from the Mixcun deposit at SAV. Andesitic rocks have Sr isotopic ratios that vary from 0.70455 to 0.70459, whereas Nd isotopic ratios vary from 0.51275 to 0.51280. The mafic enclave (sample 9320) has $^{87}Sr/^{86}Sr$ ratio of 0.70441 and $^{143}Nd/^{144}Nd$ ratio of 0.51282 (Table 4). These values of Sr isotopic ratios are typical of island arcs (Faure, 1986).

6.5 Comparison with other volcanoes

We compare the chemical signature of the TVC products to the volcanoes of the North Central American Volcanic Arc (CAVA) and the Chiapanecan Volcanic Arc (CVA) products. Mercado and Rose (1992) compared 16 andesitic rocks belonging to the TVC with rocks from volcanoes of the CVA and volcanoes of the northern part of Central American Volcanic Arc (CAVA). They concluded that the TVC rocks are associated with CAVA. In Figure 10, all TVC rocks fall within the North CAVA and CVA fields with respect to TiO_2 (0.40 -1.46 wt.%), Al_2O_3 (15.2-23.5 wt.%), CaO (4.6-9.00 wt.%), and Na_2O (2.4-4.6 wt.%) contents. The TVC and North CAVA have higher MgO (~2 wt.%) and lower K_2O (2 wt.%) and P_2O_5 (0.15 wt.%) contents compared to CVA.

Concentrations of trace elements are very similar in the three areas. The CVA is enriched in Rb (70 to 130 ppm) and Sr (831 to 1055 ppm) with respect to the TVC and North CAVA. The $^{87}Sr/^{86}Sr$ ratios decrease from 0.70409 to 0.70455

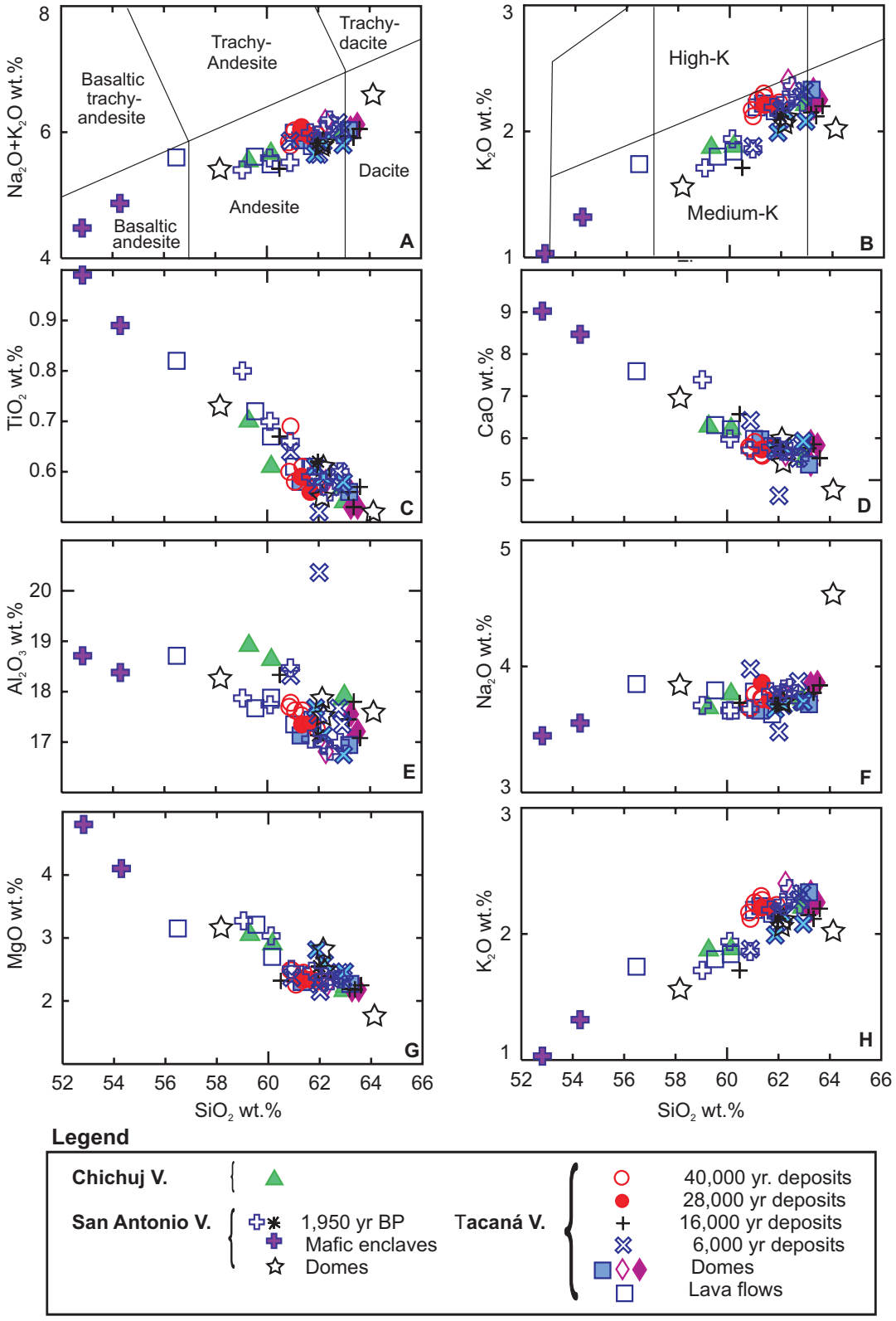

Fig. 7. Major element contents of samples from the TVC. A) Alkali vs. silica classification diagram modified after Le Bas *et al.* (1986). This shows that the mafic enclaves have basaltic-andesite composition, juvenile clasts and lava flow have andesitic composition, whereas lava flow and domes have dacitic composition. B) Silica vs. potassium plot Gill (1981), all TVC rocks fall in the field of medium-k content close to the high-k limit. C-H) Major elements vs. silica diagrams that display a straight trend between the mafic enclaves and the dacitic rocks.

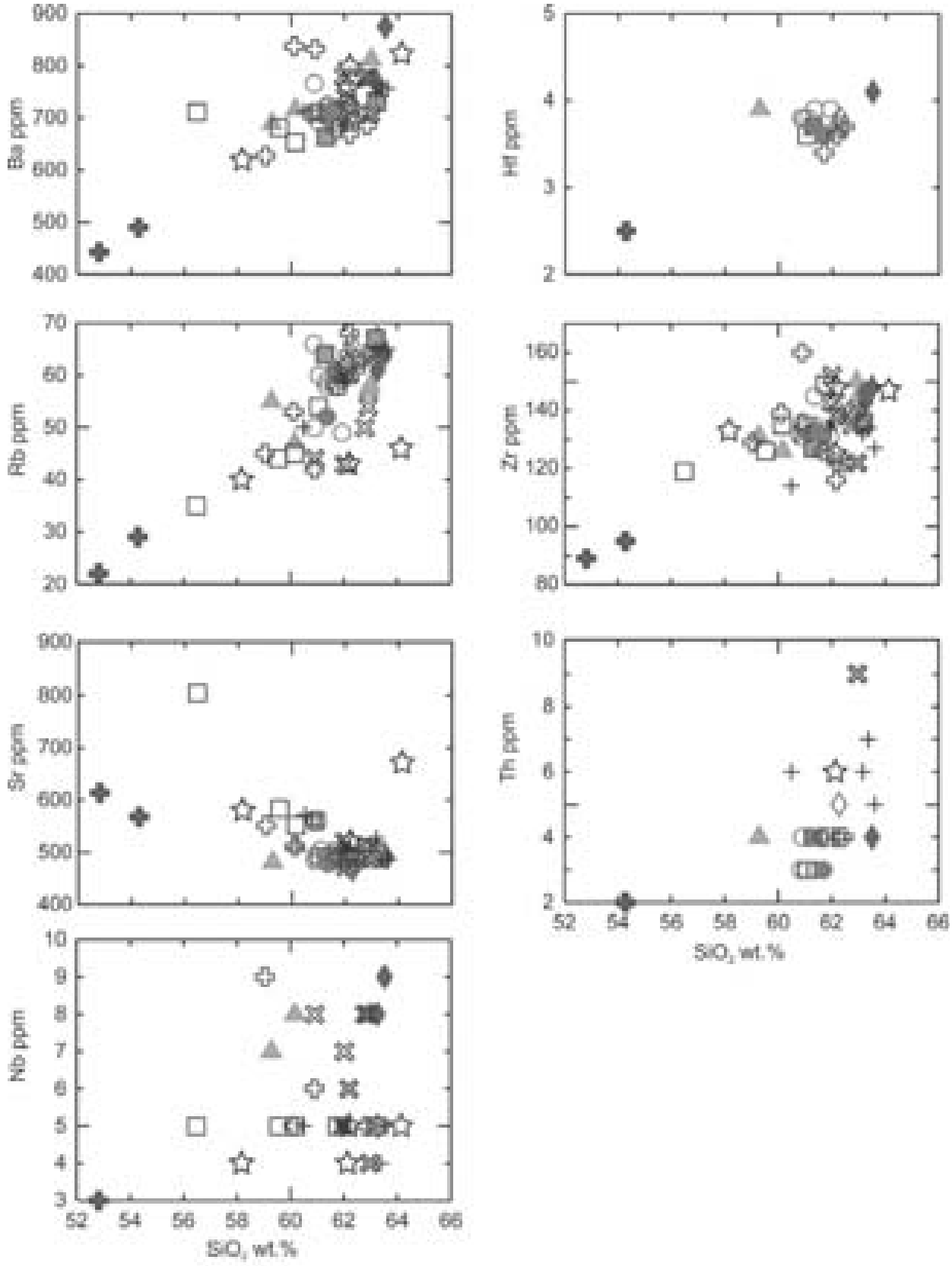

Fig. 8. Trace elements vs. silica diagrams.

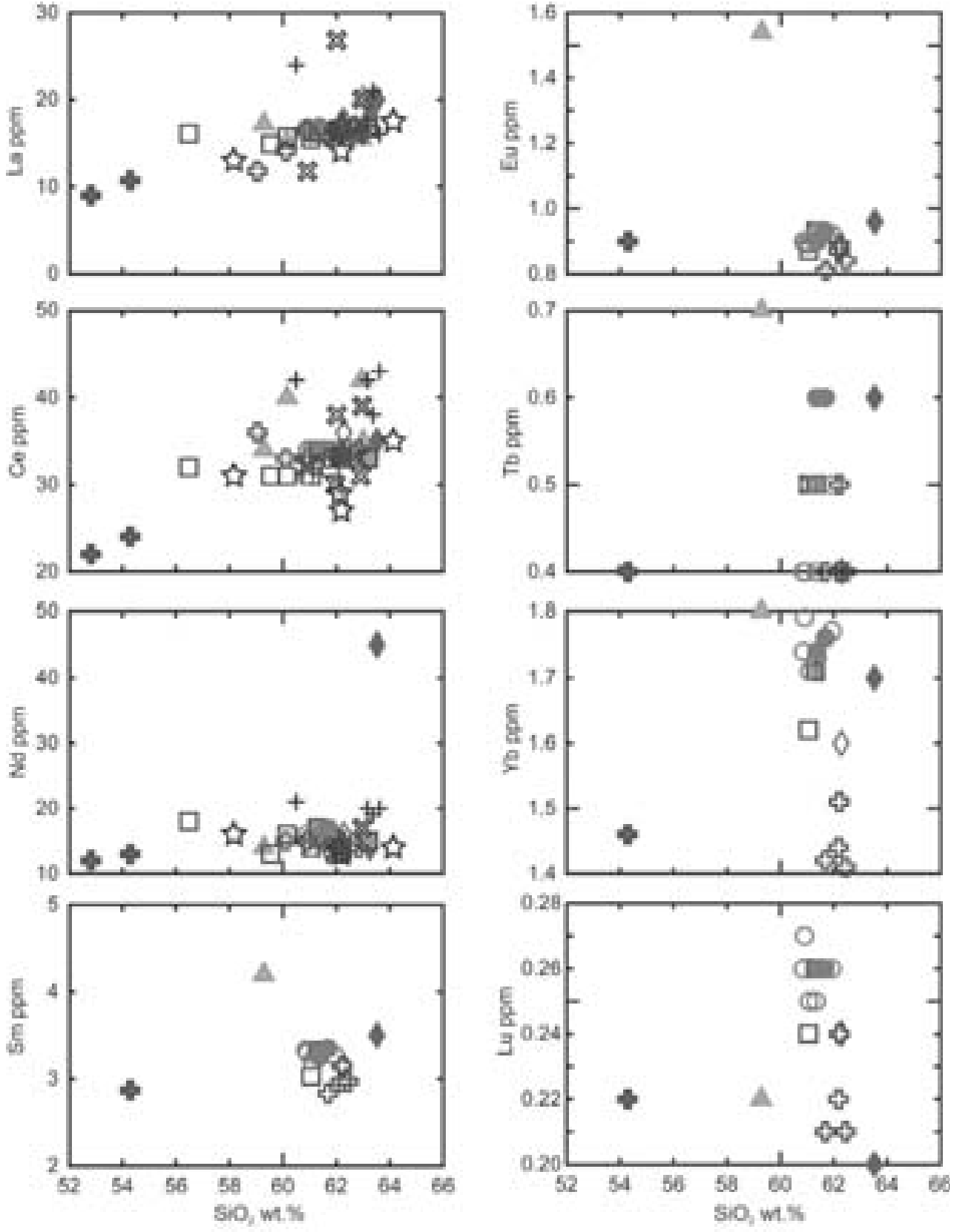

Fig. 8. Continued.

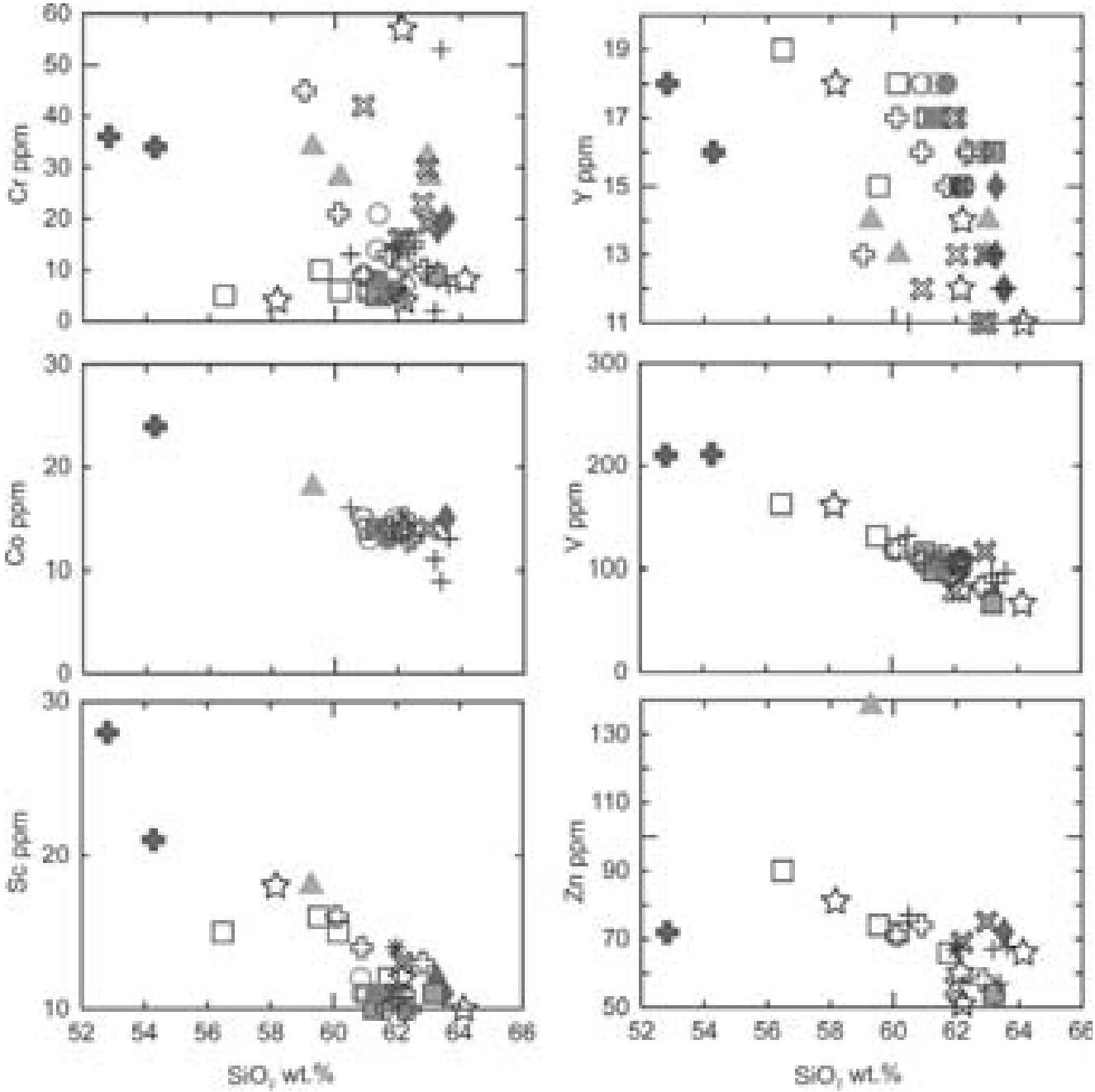

Fig. 8. Continued.

and water content increases from >6 wt.% to <3 wt.% (Mora, 2001) from El Chichón to the TVC andesite rocks. We do not observe important chemical differences between the TVC, North CAVA and CVA. They may belong to the same volcanic arc, with slight chemical variations.

Carr (1984) suggested that compositional variations in rocks erupted along arcs may record the regional effects of changing physical parameters (crustal thickness, segmentation of subducted slab, volcano spacing, and volcano size). Gill (1981) suggested that some important across-arc variations are (1) increase of K_2O and other incompatible element abundances away from the oceanic trench; (2) increase of silica range in rocks containing olivine, hornblende, and biotite phenocrysts away from the volcanic front; and (3) in some cases, a decrease in $^{87}Sr/^{86}Sr$ and $^{206}Pb/^{204}Pb$ away from the plate boundary. Increasing water and alkali content, and different source regions and extent of contamination in mag-

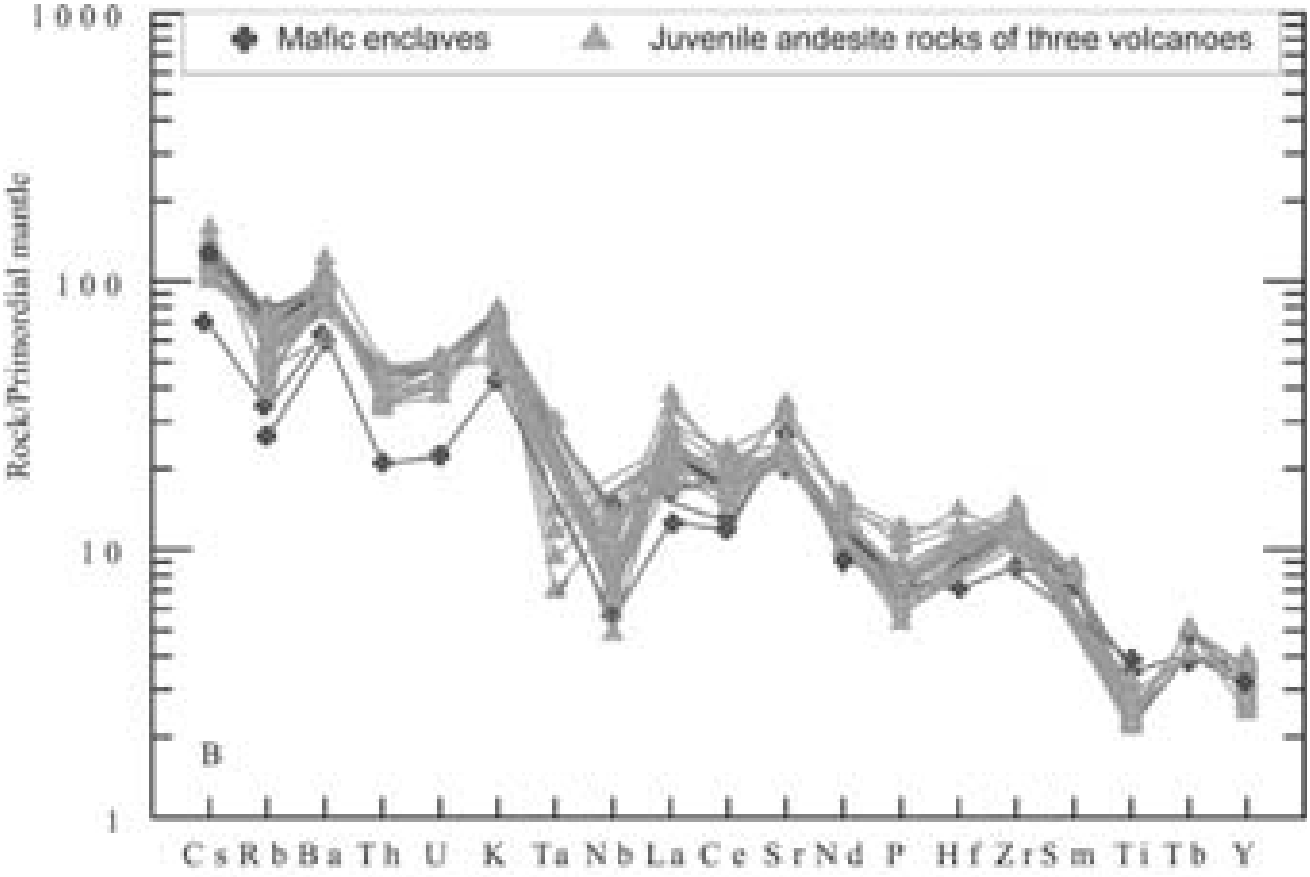

Fig. 9. Multi-element diagrams normalized to the primordial mantle (Wood 1979). Mafic enclaves are depleted in incompatible elements respect to andesites and dacites rocks.

Table 4

Isotopic ratios

SAMPLE	J	$^{87}Sr/^{86}Sr$	1σ	n	$^{143}Nd/^{144}Nd$	1σ	n	εNd	1σ	SiO_2
TAC9735a	8	0.70455	40	59	0.51275	19	55	2.26	0.37	60.94
TAC9752lj	8	0.70455	38	58	0.51276	25	58	2.38	0.49	62.68
TAC9753	8	0.70459	44	59	0.51280	26	54	3.2	0.51	60.13
TAC9875	8	0.70455	46	57	0.51279	17	56	2.89	0.33	57.59
TAC9884	9	0.70455	47	56	0.51279	37	57	2.95	0.72	64.63
TAC9320	6	0.70441	37	56	0.51282	18	57	3.57	0.35	53.86

Isotopic analyses performed on a Finnigan MAT 262 Mass Spectrometer, LUGIS, Instituto de Geofísica, UNAM. Measured values for Sr and Nd, laboratory standards are: SRM987 = 0.710233 ± 17*, La Jolla 0.511881 ± 22*.(*) = for the last two decimals units, n = number of analyses. Analyses performed by T. Treviño, G. Solís, J. Morales, and M. Hernández.

mas away from the trench are often called upon to explain these across-arc variations (Sakuyama, 1977; Gill, 1981). Halsor and Rose (1988) describe compositional differences in paired volcanoes, reflecting variations in crustal thickness, and providing insight into across-arc variations and closely-spaced subvolcanic plumbing systems. The CVA shows enrichment in water, K_2O, Rb, and Sr, and decrease in $^{87}Sr/^{86}Sr$ that ratios may be related to its location at 370 km from the

trench, where there is a large variation in depth, dip of the seismic zone, convergence rate, age of underthrusting oceanic crust, and basement type respect to North CAVA and TVC. Luhr *et al.* (1984) relate the enrichments to the large distance from El Chichón to the Middle American Trench, or to the subduction of the Tehuantepec Ridge, a major fracture zone of the Cocos Plate, beneath Chiapas.

7. DISCUSSION

The NE-SW alignment of the three volcanic edifices (older CHV, TV, and younger SAV) forming the TVC suggests a southwestern migration of volcanism. These volcanoes have been the focus of monotonous andesitic magmas with minor fluctuations to basaltic-andesitic or dacitic magmas erupting through time. O'Hara (1977) suggested that eruption of monotonous andesitic composition represents products of a long-residence time magma system with a steady-state composition. Halsor and Rose (1988) describe magmas in the Tolimán-Atitlán volcano undergoing long periods of stagnation interrupted by mafic injection and rapid eruption. The presence of phenocrysts (up to 2 cm) and microphenocrysts, with euhedral forms of the same mineral phases in the TVC andesitic products also provides indirect evidence that a long-residence magma was established beneath the volcano (O'Hara, 1977). This evidence is strengthened by the homogeneous chemical composition of the andesitic to dacitic TVC products.

The presence of mafic enclaves of basaltic-andesitic composition with rounded, elongated, and ellipsoidal forms, interstitial glass, and chilled margins with respect to the andesitic host rock, suggest that batches of more basic magma were periodically injected from depth. This compositional variation was observed in the San Antonio volcano products.

The repeated arrival of mafic magmas to the base of the TVC magma chamber filled with a pre-existing crystal-rich liquid, causes mixing of two magmas to produce a hybrid andesitic magma that later crystallizes. This evolution produces a repeated emission of evolved andesitic and dacitic magmas at TVC. The scarcity of erupted mafic magmas at the TVC might indicate that a complete homogenization of magma is forming an andesitic hybrid, which evolves growing reverse and oscillatory plagioclase phenocrysts (Figure 11 A-B).

The mafic enclaves sampled in the SAV products have slightly chilled margins and plastic rounded forms. Together with the compositional gap observed in the major and trace elements of the SAV products this suggests a later injection of mafic magma in the magma chamber (Figure 11 C-E). This mafic magma came into contact with a crystal-rich andesitic magma stagnating at depth (Macías *et al.*, 2000). Interaction between these two magmas was fast; thus so incomplete mixing occurred, producing reaction rims (Fe-Ti oxides) on amphibole phenocrysts. It destabilized the magma system, which eventually culminated with a Peléan eruption 1950 yr ago.

During the time that the hybrid magma resided in the chamber, probably a slight assimilation of the basement may have occurred.

8. CONCLUSIONS

The TVC consists of three NE-SW aligned volcanoes from the oldest to the youngest, *i.e.* Chichuj, Tacaná, and San Antonio. The most abundant products associated with the eruptive activity of these volcanoes are block-and-ash-flow deposits, and lesser amounts of lava flows and domes. The lava flows and domes are andesitic and dacitic, while the juvenile clasts of the pyroclastic flow deposits are andesites. The more mafic rocks associated to this complex are mafic enclaves of basaltic-andesite composition hosted in andesites of the SAV, plus some gabbroic intrusions in the basement. The analyzed rocks have a porphyritic texture with glass in the groundmass as an indication of incomplete crystallization. The most common mineral association is plagioclase, pyroxene, and amphibole. Amphibole phenocrysts are more abundant in SAV > TV > CHV. The mafic enclaves with slightly chilled margins, irregular forms, and intersertal texture are an evidence of mafic magma injection into an andesitic or dacitic magma chamber.

The mineral disequilibrium textures and reverse zoning of phenocrysts suggest that repeated injection of basaltic-andesite magmas into an andesitic magma chamber has taken place beneath the TVC through time. Mixing between these two magmas has produced a hybrid andesitic magma that predominates by volume among the eruptive products of the TVC over time. The particular case of the SAV andesites, which host basaltic-andesite enclaves, represents an incomplete mixing process produced by the injection of hot mafic magma into a crystal-rich stagnant andesitic melt. This injection triggered a Peléan-type eruption 1950 yr ago.

ACKNOWLEDGEMENTS

This research was supported by CONACYT grants (38586-T to J. L. M., and 32312-T to J. M. E.), and CONACYT-CNR bilateral project to J. L. M. The help of several people is gratefully acknowledged: F. Olmi provided technical support during the microprobe analyses performed at C. N. R at Universita degli Studi di Firenze, G. Valdéz, T.

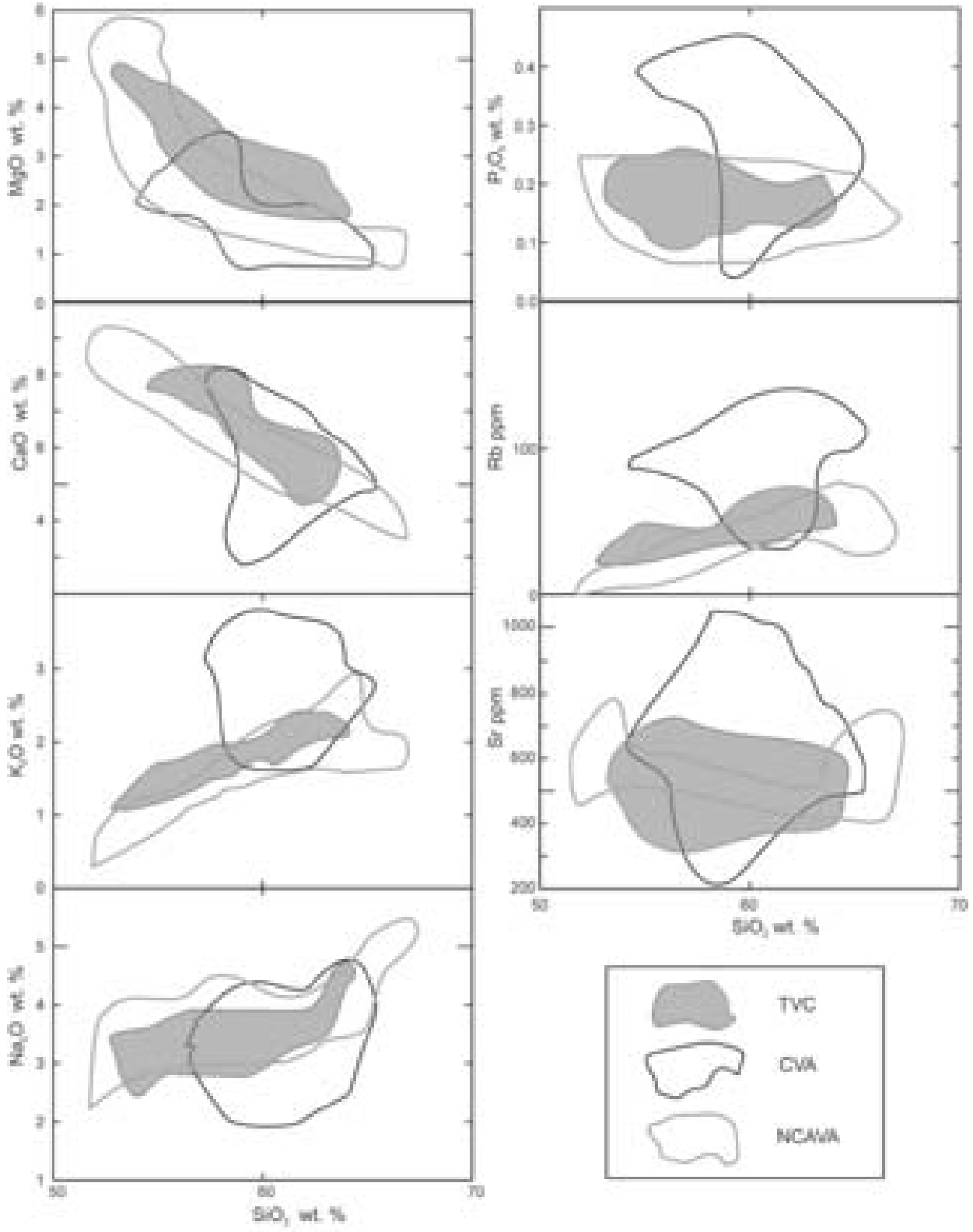

Fig. 10. Major elements content comparison diagrams between CHVA, Chiapanecan Volcanic Arc composed by El Chichón, Tzontehuitz and Nicolás Ruiz volcanoes (Luhr *et al.*, 1984; McGee *et al.*, 1987; Espíndola *et al.*, 2000). TVC, Tacaná Volcanic Complex composed by Chichuj, Tacaná and San Antonio volcanoes (Mercado and Rose, 1992; Macías *et al.*, 2000; Mora, 2001). NCAVA, North Central America Volcanic Arc composed by Tajumulco, Santa María, Santiaguito and Chicabal (Carr and Rose, 1987).

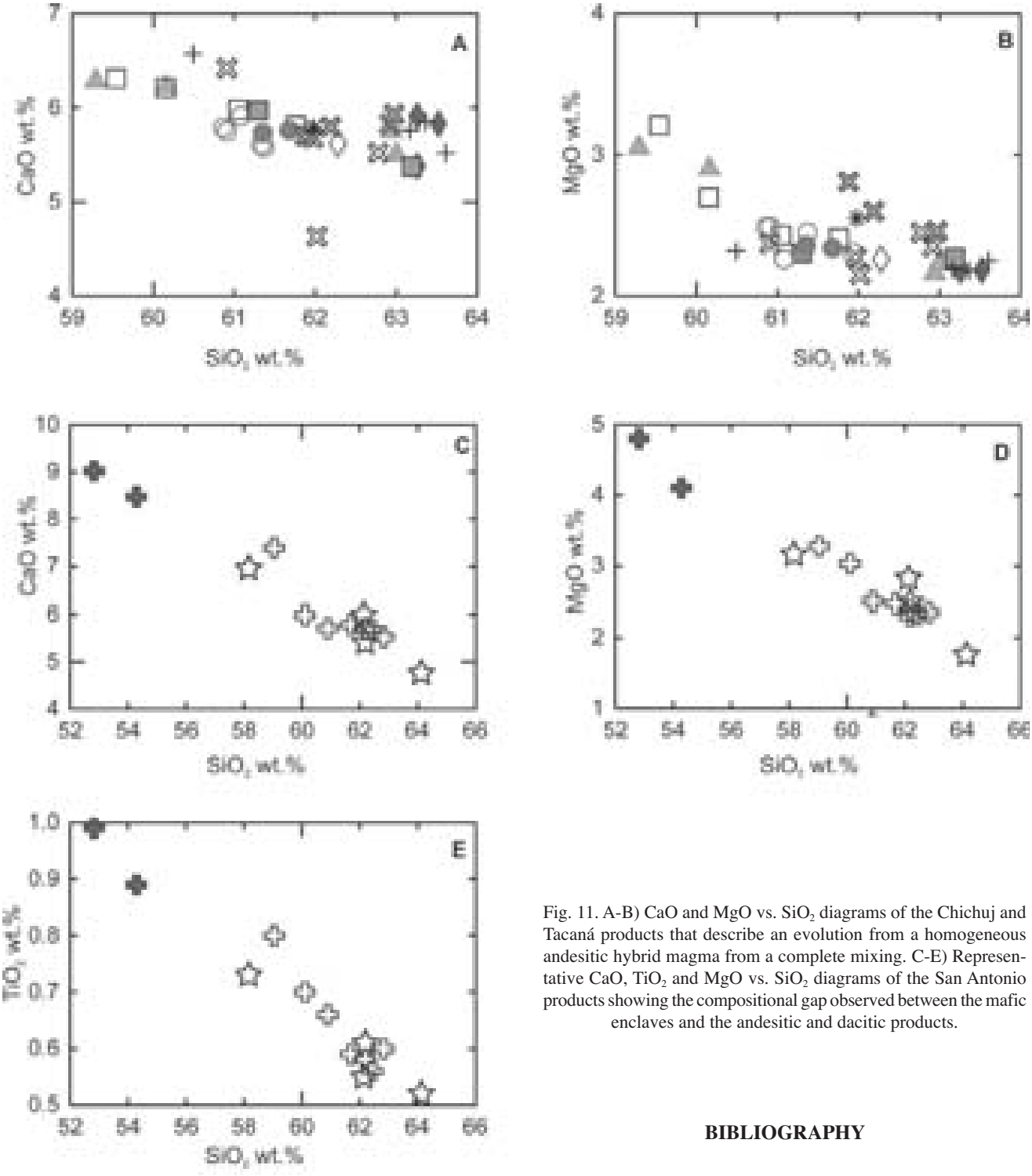

Fig. 11. A-B) CaO and MgO vs. SiO_2 diagrams of the Chichuj and Tacaná products that describe an evolution from a homogeneous andesitic hybrid magma from a complete mixing. C-E) Representative CaO, TiO_2 and MgO vs. SiO_2 diagrams of the San Antonio products showing the compositional gap observed between the mafic enclaves and the andesitic and dacitic products.

Hernández, G. Solís, and P. Schaff provided technical and instrumental support at Instituto de Geofísica de la UNAM. We acknowledge the reviews by G. Carrasco and an anonymous reviewer.

BIBLIOGRAPHY

BENCE, A. E. and A. L. ALBEE, 1968. Empirical correction factors for the electron microanalyses of silicates and oxides. *Geology 76,* 382-483.

BERGEAT, A., 1894. Zur Kenntnis der jungen Eruptivgesteine der Republik Guatemala: *Zeitschr. Deutsch. Geol. Gesell. Berlin, Bd. 46,* 131-157.

BÖSE, E., 1903. Los temblores de Zanatepec, Oaxaca, a fines de septiembre de 1902 y el estado actual del Volcán Tacaná, Chiapas. Boletín del Instituto de Geología, México, parergones, 1, 1, 1-25.

BÖSE, E., 1905. Reseña acerca de la geología de Chiapas y Tabasco. Boletín del Instituto de Geología, México, 20, 6-103.

CARR, M. J., 1984. Symmetrical and segmented variation of physical and geochemical characteristics of the Central American volcanic front. *J. Volc. Geotherm. Res., 20,* 231-252.

CARR, M. J. and W. I. ROSE, 1987. CENTAM-a data base of analyses of Central American volcanic rocks. *J. Volcanol. Geotherm. Res., 33,* 239 240.

CARR, M. J., W. I. ROSE JUNIOR and R. E. STOIBER, 1982. Central America. *In:* Orogenic Andesites, R. S. Thorpe (ed.) John Wiley, p149-166.

DAMON, P. E. and E. MONTESINOS, 1978. Late Cenozoic Volcanism and Metallogenesis over an active Benioff Zone in Chiapas, Mexico. Arizona Geological Society Digest, Xl, 155-168.

DAMON, P. E. and G. P. SALAS, 1975. Dating of Mesozoic-Cenozoic metallogenetic provinces within the Republic of Mexico (1965-1975): Cooperative research project between Laboratory of Isotope Geochemistry, Dept. of Geosciences, University of Arizona and the Consejo de Recursos Minerales, Interim Report, unplublished.

DE CSERNA, Z., J. J. ARANDA-GÓMEZ and L. M. MITRE SALAZAR, 1988. Mapa fotogeológico preliminar y secciones estructurales del volcán Tacaná. UNAM, Inst. Geología, Carta Geol. y Min., No. 7, 1pp.

DE LA CRUZ, V. and R. HERNÁNDEZ, 1985. Estudio geológico a semidetalle de la zona geotérmica del volcán Tacaná, Chis. Informe 41/85, Departamento de Exploración, Comisión Federal de Electricidad, 27pp.

DE VRIES and JENKINS, 1971. Spettrometria a raggi X in practical 193pp.

DONNELLY, T. W., G. S. HORNE, R. C. FINCH and E. LÓPEZ-RAMOS, 1990. Northern Central America: the Maya and Chortis blacks. *In:* Dengo, G., Case, D.J. (eds). The Geology of North America: the Caribbean Region, 37-76.

ESPÍNDOLA, J. M., J. L. MACÍAS and M. F. SHERIDAN, 1993. El Volcán Tacaná: un ejemplo de los problemas de evaluación del riesgo volcánico. Actas del Simposio Internacional sobre Riesgos Naturales e Inducidos en los grandes Centros Urbanos de América Latina. Serie Ciencia, 5, 62-71.

ESPÍNDOLA, J. M., F. M. MEDINA and M. DE LOS RÍOS, 1989. A C-14 age determination in the Tacaná volcano (Chiapas, Mexico) *Geofís. Int., 28,* 123-128.

ESPÍNDOLA, J. M., J. L. MACÍAS, R. I. TILLING and M. F. SHERIDAN, 2000. Volcanic history of El Chichón Volcano (Chiapas, Mexico) during the Holocene, and its impact on human activity. *Bull. Volcanol., 62,* 90-104.

FAURE, G., 1986. Principles of isotope geology. Second edition, John Wiley and Sons, N.Y.

GILL, J. B., 1981. Orogenic, Andesites and Plate Tectonics. Springer and Verlag Publication Berlino, 390pp.

GUZMÁN-SPEZIALE, M., W. D. PENNINGTON and T. MATUMOTO, 1989. The triple junction of North America, Cocos and Caribbean plates: Seismicity and tectonics. *Tectonics, 8,* 981-997.

HALSOR, S. P. and W. I. ROSE, 1988. Common characteristics of paired volcanoes in Northern Central America. *J. Geophys. Res., 93, B5,* 4467-4476.

IRVINE, T. N. and W. R. A. BARAGAR, 1971. A guide to the chemical classification of the common volcanic rocks. *Can. J. Earth Sci., 8,* 523-548.

LE BAS, M. J., R. W. LE MAITRE, A. STREICKENSEN and B. ZANETTIN, 1986. A chemical classification of volcanic rocks on the total Alkali-Silica Diagramm. *J. Petrol., 27,* 745-750.

LEAKE, B. E., A. R. WOOLLEY, C. E. S. ARPS, W. D. BIRCH, M. C. GILBERT and J. D. GRICE, 1997. Nomenclature of amphiboles: report of the subcommittee on amphiboles of the International Mineralogical Association, commission on new minerals and mineral names. *American Mineralogist 82,* 1019-1037.

LUHR, J. F., I. S. E. CARMICHAEL and J. C. VAREKAMP, 1984. The 1982 eruptions of El Chichón Volcano, Chiapas, Mexico: mineralogy and petrology of the an-

hydrite bearing pumices. *J. Volcanol. Geotherm. Res., 23,* 69-108.

MCGEE, J. J., R. I. TILLING *et al*., 1987. Petrologic characteristics of the 1982 and pre 1982 eruptive products of El Chichón volcano, Chiapas, Mexico. *Geofís. Int., 26,* 85-10.

MACÍAS, J. L., J. M. ESPÍNDOLA, A. GARCÍA-PALOMO, K. M. SCOTT, S. HUGHES and J. C. MORA, 2000. Late Holocene Peléan Style Eruption at Tacaná Volcano, Mexico Guatemala: Past, Present, and Future Hazards. *Geol. Soc. Amer. Bull., 112,* 1234-1249.

MERCADO, R. and W. I. ROSE, 1992. Reconocimiento geológico y evaluación preliminar de la peligrosidad del volcán Tacaná, Guatemala/México. *Geofís. Int., 31,* 205-237.

MORA, J. C., 2001. Studio Vulcanologico e Geochimico del Vulcano Tacaná Chiapas, Messico. PhD Thesis, Universitá Degli Studi di Firenze, Italy, 147pp.

MÚJICA, R., 1987. Estudio petrogenético de las rocas ígneas y metamórficas en el Macizo de Chiapas. Reporte Instituto Mexicano del Petróleo, C-2009, 1-47.

MÜLLERRIED, F. K. G., 1951. La reciente actividad del volcán de Tacaná, Estado de Chiapas, a fines de 1949 y principios de 1950. Boletín Instituto de Geología, UNAM, México, 1-28p.

NAKAMURA, N., 1974. Determination of REE, Ba, Fe, Mg, Na and K in carbonaceous and ordinary chondrites. *Geochim. Cosmochim. Acta. 38,* 757-773.

O'HARA, M. J., 1977. Geochemical evolution during fractional crystallization of a periodically refilled magma chamber. *Nature 266,* 503-507.

ORDOÑES, E., 1905. Descripción de las rocas. *In:* Böse, E., Reseña acerca de la geología de Chiapas y Tabasco. Inst. Geol. México, 20, 101-113.

PATIÑO, L. C., M. J. CARR and M. D. FEIGENSON, 2000. Local and regional variations in Central American arc lavas controlled by variations in subducted sediment input. *Contrib. Mineral. Petrol., 138*, 265-283.

ROSE, JR. W. I., 1972a. Notes on the 1902 eruption of Santa María Volcano, Guatemala. *Bull. Volcanol, 36,* 29-45p.

ROSE, JR. W. I., 1972b. Santiaguito volcanic dome, Guatemala. *G.S.A. Bull., 83,* 1413 1434.

SAKUYAMA, M., 1977. Lateral variations of H2O contents in Quaternary magma of northeast Japan. *Bull. Volcanol. Soc. Jpn., 22,* 263-271.

SHAPIRO, L. and W. W. BRANNOCK, 1962. Rapid analyses of silicate, carbonate and phosphate rocks. *Geological Survey Bull. 1144,* 1-55.

STORMER, J. C., 1983. The effects of recalculation on estimates of temperature and oxygen fugacity from analyses of multicomponent iron-titanium oxides. *Amer. Mineral., 68,* 586-594.

WHITE, 1991. Tectonic implications of upper-crustal seismicity in Central America. *In:* Neotectonics of North America, edited by D. B. Slemmons, E. R. Engdahl, M. D. Zoback, and D. D. Blackwell, 323-338p, Gelogical Society of America, Boulder, CO.

WOOD, A., 1979. A variably veined sub-oceanic upper mantle-genetic significance for mid-ocean ridge basalts from geochemical evidence. *Geology, 7,* 499-503.

J. C. Mora[1,3*], J. L. Macías[1], A. García-Palomo[2], J. L. Arce[1], J. M. Espíndola[1], P. Manetti[3], O. Vaselli[3] and J. M. Sánchez[4]

[1] Instituto de Geofísica, UNAM, Coyoacán, 04510 México D.F., México

Email: jcmora@tonatiuh.igeofcu.unam.mx

[2] Departamento de Geología Regional, Instituto de Geología, UNAM, Coyoacán, 04510 México D.F.

[3] Dipartimento di Scienze della Terra, Universitá degli Studi di Firenze, Firenze, Italia

[4] Centro Interdisciplinario de Investigaciones y Estudios sobre Medio Ambiente y Desarrollo, (CIIEMAD), IPN, México, D.F.